https://doi.org/10.5194/wes-2023-82
Preprint. Discussion started: 10 November 2023

eawe european academy of wind energy
Open Access WIND ENERGY SCIENCE DISCUSSIONS

Estimating the technical wind energy potential of Kansas that incorporates the atmospheric response for policy applications

Jonathan Minz[1,5], Axel Kleidon[1], and Nsilulu T. Mbungu[2,3]

[1]Biospheric Theory and Modelling Group, Max Planck Institute of Biogeochemistry, Jena, Germany
[2]Department of Electrical Engineering, Tshwane University of Technology, Pretoria, South Africa
[3]Department of Electrical Engineering, University of Sharjah, Sharjah, United Arab Emirates
[5]Institute of Physics and Meteorology, University of Hohenheim, Stuttgart, Germany

Correspondence: Jonathan Minz (jminz@bgc-jena.mpg.de)

Abstract. Energy scenarios and transition pathways require estimates of achievable technical wind energy potentials to evaluate the integration of large scale wind energy into the electrical grid. Technical potential refers to the projected electrical generation from regional scale wind turbine deployments, while accounting for the actual area available, turbine characteristics, losses from inter-turbine interactions and energy conversion. These are distinct from resource potentials for wind park planning and layout and are estimated using a typical approach in which the turbines' power curves are forced by either observed or modelled hub-height wind speeds. This approach, which we refer to as the standard approach, implicitly assumes minimal impacts of large scale wind energy generation on the regional wind resource and, thus, fixes the impacts of associated generation losses on technical potential to 10%. However, the depletion of wind resource or the reduction in wind speed scales with the total capacity installed within the deployment. Therefore, the standard approach overestimates the technical potential relative to estimates that are derived using Weather Research and Forecasting (WRF) models with interactive wind farm parameterizations. Here, we test the extent to which these impacts of wind resource depletion on technical potential can be captured by using our KE Budget of the Atmosphere (KEBA) approach over Kansas(USA) for a range of hypothetical deployment scenarios. KEBA estimates wind resource depletion impacts by accounting for the kinetic energy (KE) removed by the turbines from the boundary layer budget. We first evaluate its ability to replicate the numerically projected diurnal variations in wind resource depletion and then account for the change in technical potential. KEBA captures the projected diurnal variations in to within 5 and 22% during day and night, respectively, whereas the standard approach projects no impact. Nighttime variation is underestimated by KEBA due to stability effects. Overall, KEBA is able to reproduce the WRF simulated technical potential of Kansas within about 10%, with the WRF potential being around 50% lower than the standard approach. Despite this, the WRF estimated potential of Kansas remains about 3 to 5 times the total energy consumed in the state in 2018. KEBA is a simple yet adequate approach to estimating technical potentials, and highlights the wind resource depletion effects that will occur from regional-scale wind deployment.

https://doi.org/10.5194/wes-2023-82
Preprint. Discussion started: 10 November 2023

eawe european academy of wind energy
Open Access WIND ENERGY SCIENCE DISCUSSIONS

1 Introduction

Estimates of technical wind energy potential are important for the design of energy transition pathways towards a future sustainable energy system (Prakash et al., 2019; Ruijgrok et al., 2019; GEA, 2012; IEA, 2021). They are inputs to integrated assessment models that deploy large scale wind and solar and evaluate the impact of the integration of these variable sources into the electrical grid (Eurek et al., 2017). Technical potentials are defined as theoretical estimates of electrical generation from hypothetical regional scale wind turbine deployments while accounting for areas that are actually available for wind energy development, wind turbine characteristics and, losses arising from inter-turbine interactions and energy conversion (Hoogwijk et al., 2004; McKenna et al., 2022; Manwell et al., 2010). The actual area available for wind energy development pertains to that over which wind turbines can be installed after accounting technical, ecological and social constraints (McKenna et al., 2022). Technical potentials pertain specifically to the projected generation from future large scale wind turbine deployments and are highly policy relevant (McKenna et al., 2022). A significant part of the policy relevance stems from the fact that technical potentials are significant control on the economic costs of wind energy development (Blanco, 2009; Ragheb, 2017).

These resource potential estimates are especially distinct from the resource estimation performed for wind park planning and layout. The large scale at which these are estimated, typically spanning thousands of square kilometers with hundreds of GWs in deployed capacity, means that the detailed approaches used in wind park planning and layout such as the Weather Research Forecasting (WRF) (Blahak and Wetter-Jetzt, 2010; Fitch et al., 2012; Volker et al., 2015; Boettcher et al., 2015), Computational Fluid Dynamical (Wu and Porté-Agel, 2015) and engineering wake models (Katic et al., 1986; Frandsen et al., 2006; Pedersen et al., 2022) are not employed. The use of such comprehensive, numerical models in energy scenario analysis is impeded by their need for high performance computing infrastructure and subject matter expertise (Staffell and Pfenninger, 2016). Thus, the typical approach for estimating technical potential for application in energy scenario analyses and integrated assessment modelling relatively straighforward in comparison to the more comprehensive approaches mentioned above. In this analysis, we use the term standard approach to refer specifically to the this approach and not those employed for resource assessment for wind park planning and layout which is outside the scope of this study.

The standard approach to estimating technical potential is to force a single wind turbine's power curve with observed or modelled time series of hub-height wind speeds. The potential then is a function of regional wind resource or wind speeds, turbine power curve and the total number of wind turbines within the deployment area (Hoogwijk et al., 2004; Archer and Jacobson, 2005; Lu et al., 2009; Schallenberg-Rodriguez, 2013; Eurek et al., 2017; Enevoldsen et al., 2019). This approach differs from those typically employed in high resolution evaluations of wind park planning and layout, primarily, in its handling of energy generation and conversion losses. The standard approach fixes these losses to 10% (Hoogwijk et al., 2004; Schallenberg-Rodriguez, 2013; Eurek et al., 2017). This stems from the implicit assumption that large scale wind energy generation minimally impacts the regional wind resource. This leads to an expectation of a linear relationship between technical potential and capacity deployed. Further, it is implied that efficiency of the wind turbine deployment measured in terms of the capacity factor or the ratio of actual to rated wind turbine generation remains constant relative to the size of the deployed capac-

https://doi.org/10.5194/wes-2023-82
Preprint. Discussion started: 10 November 2023

eawe european academy of wind energy
Open Access WIND ENERGY SCIENCE DISCUSSIONS

ity. Therefore, larger deployed capacities at the regional scale with better turbines are expected to always lead to a proportionate increase in technical potential(Wiser et al., 2016).

However, meso and synoptic scale simulations of technical potentials from regional scale deployments using numerical models of the atmosphere like WRF and Global Circulation models show that the standard approach significantly overestimates technical potential and capacity factors when wind energy is intensively used at large scales (Adams and Keith, 2013; Miller et al., 2015; Miller and Kleidon, 2016; Volker et al., 2017; Badger et al., 2020; Kleidon and Miller, 2020; Jacobson and Archer, 2012). These studies highlight that technical potential and capacity factors do not scale linearly or remain constant, respectively, with the deployed capacity. This sub-linear increase in technical potential and the erosion of the capacity factor results from the depletion of regional wind resource (Miller et al., 2015; Miller and Kleidon, 2016; Kleidon and Miller, 2020; Kleidon, 2021) because wind turbines remove kinetic energy (KE) from the boundary layer winds to generate electricity. This effect is borne out in observation data.

Wind resource depletion or the reduction in wind speeds behind wind turbine deployments has been observed in a variety of measurement data from currently operating wind farms (Rajewski et al., 2013; Bodini et al., 2017; Lundquist et al., 2014; Hasager et al., 2015; Platis et al., 2018; Ahsbahs et al., 2020; Nygaard and Newcombe, 2018; Nygaard et al., 2020). Referred also to as wakes, wind speed reductions can extend up to 50 km behind operating wind farms (Cañadillas et al., 2020; Lundquist et al., 2018). The reduced wind speeds interact with and reduce the electrical generation from downstream wind farms (Méchali et al., 2006; Schneemann et al., 2020; Maas and Raasch, 2021; Akhtar et al., 2021). Numerical simulations of this phenomenon also compare reasonably well with the observations (Mirocha et al., 2015; Aitken et al., 2014; Siedersleben et al., 2018; Fischereit et al., 2021). Thus, it can be assumed that the impact of wind resource depletion on wind energy generation will persist as the scale of wind turbine deployment is increased and, thus, must be incorporated into energy scenario analyses. For these to be incorporated in to energy scenario modelling, it is necessary to scale the impacts up to the proposed regional deployment scales while balancing the constraints on computational complexity and ease of implementation highlighted by Staffell and Pfenninger. This means that the key physics that shape the regional wind resource depletion and its impact on technical potential be understood. For this we need to look at how kinetic energy is generated and transported towards the surface before it can be extracted by wind turbines.

The winds of the large-scale circulation and KE associated with their mean flow are predominantly generated in the free atmosphere by differences in potential energy due to differential solar radiative heating (Peixoto and Oort, 1992; Kleidon, 2021). This KE is transported vertically downwards into the boundary layer, the lowest layer of the atmosphere where most of the KE is dissipated (Stull, 2009). The turbines extract some of the KE which would otherwise have been dissipated by surface friction. Since the rate at which KE is transported into the boundary layer is limited, it leads to a fixed KE budget being available for driving movement within the boundary layer(Kleidon and Miller, 2020). This means that the extraction of KE by a large number of wind turbines leads to less KE being available for the motion of the winds. Put another way wind turbines generate electricity by depleting the boundary layer KE resource. As a result, larger rates of KE extraction from a fixed KE budget causes slower winds and reduced capacity factors (Miller et al., 2011). This is supported by mesoscale WRF simulations, which show that technical potentials from onshore deployments larger than 100 km^2 are limited to yields of about

https://doi.org/10.5194/wes-2023-82
Preprint. Discussion started: 10 November 2023

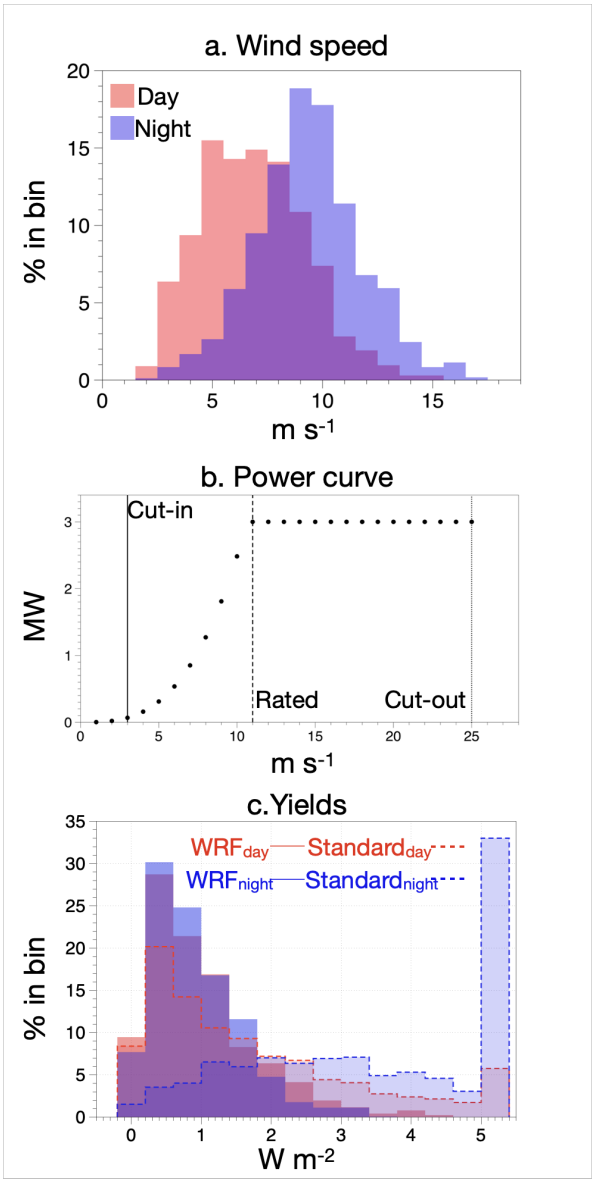

Figure 1. (a) Distribution of wind speeds averaged over a prospective deployment area in Kansas, central US, for daytime (red) and nighttime (blue) in the absence of wind turbines. (b) The power curve for a Vestas V112 3MW wind turbine used in this study. It does not generate electricity for wind speeds below the "cut-in" (3 m s^{-1}, solid black line) and above the "cut-out" wind speed (25 m s^{-1}, dotted black line). Yields vary with the cube of wind speeds below the "rated" wind speed (11 m s^{-1}, stippled black line) but remain at capacity above it. (c) Deployment yields during daytime (red) and nighttime (blue) for the 5 MW km^{-2} scenario from an interactive WRF simulation (solid, "WRF"), and using the standard approach (dashed outlines). WRF estimates that the total deployment yield during the day (WRF_{day} = 63 GW) is higher than nighttime (WRF_{night} = 42 GW), while the standard estimate yields higher potentials and the opposite response ($Standard_{day}$ = 109 GW, $Standard_{night}$ = 159 GW). Data taken from Miller et al. (2015).

https://doi.org/10.5194/wes-2023-82
Preprint. Discussion started: 10 November 2023

eawe european academy of wind energy
Open Access WIND ENERGY SCIENCE DISCUSSIONS

1.1 W m^{-2} for very intensive turbine densities (Adams and Keith, 2013; Miller and Kleidon, 2016; Jacobson and Archer, 2012; Marvel et al., 2012; Gustavson, 1979; Wang and Prinn, 2010, 2011; Volker et al., 2017), which contrast with standard estimates ranging from 2-6 W m^{-2}(Jacobson and Delucchi, 2011; Jacobson and Archer, 2012; Lu et al., 2009; Archer and Jacobson, 2005; Edenhofer et al., 2011; Capps and Zender, 2010). At the maximum potential, wind speeds are estimated to slow by 42%, while capacity factors reduce by $\sim$ 50% relative to the standard estimate (Miller et al., 2015; Volker et al., 2017). A mean of 1.1 W m^{-2} implies electricity generation of $\sim$ 900 - 1900 TWh yr^{-1} if all the available area for wind energy in a windy area like Kansas (100,000 - 200,000 km^{-2}) is covered with wind turbines. These generation potentials are about a third lower than the standard expectation of 2000 - 3000 TWh yr^{-1} (Brown et al., 2016; Lopez et al., 2012). Thus, the standard approach to technical potential estimation in energy scenario analyses needs to incorporate the effects of wind speed reductions arising from limitations imposed by the atmospheric KE budgets.

A simple yet physical approach to deriving technical potential estimates that includes the effects of KE removal on wind speeds is to constrain the wind speeds and turbine yields with an explicitly defined KE budget of the atmospheric boundary layer. In this approach, known as the Kinetic Energy Budget of the Atmosphere (KEBA, Kleidon and Miller (2020)), first the budget available to the deployment is estimated from the sum of the vertical and horizontal KE fluxes over the deployment. The vertical component represents the KE input into the boundary layer from the free atmosphere while the horizontal component represents the boundary layer wind flow. Both rates can be estimated from wind speed observations, but also depend on boundary layer height and surface friction. The reduction in wind speeds is estimated by accounting for the removal of KE from the budget. The slower wind speeds are then used to estimate turbine yields(Kleidon and Miller, 2020). This approach has previously been shown to compare well against numerical weather forecasting simulations of wind turbine deployments in idealized onshore weather conditions(Kleidon and Miller, 2020) and in real weather conditions in offshore areas in the German Bight of the North Sea (Badger et al., 2020). The goal here is to test this approach further in a realistic onshore region to understand the limits of its application for it to be used in technical potential estimation for energy scenario analyses.

In this study, we will use this approach to evaluate a seemingly counter-intuitive result (Fig. 1) reported by previous numerical simulations of hypothetical large-scale wind turbine deployment scenarios in Kansas, central US, under realistic weather conditions (Miller et al., 2015). These simulations showed that wind speeds are typically 40% lower during the day than at night (Fig. 1a), but overall daytime electrical yields were about 50% higher than nighttime (Fig. 1c). This is an important result to evaluate with KEBA since the standard approach would estimate the opposite, higher nighttime yields due to higher wind speeds. The result can be understood when one accounts for the effect of lower boundary layer heights and reduced mixing at night, which reduces the size of the kinetic energy budget (Fig. 2). As a result the KE removal by the wind turbines has a stronger effect on wind speed reductions at night (Fitch et al., 2013a; Abkar et al., 2015). During the day, because the KE budget is larger, this depletion effect is proportionally smaller. Solar insolation drives vertical convection and the vertical growth of the boundary layer, resulting in higher downward replenishment of KE from the free atmosphere and a larger reservoir of KE in the boundary layer. The absence of solar-driven convection at night leads to stratified or stable conditions that restricts vertical KE replenishment. This leads to greater reduction in wind speeds at night compared to the the day, and therefore lower

https://doi.org/10.5194/wes-2023-82
Preprint. Discussion started: 10 November 2023

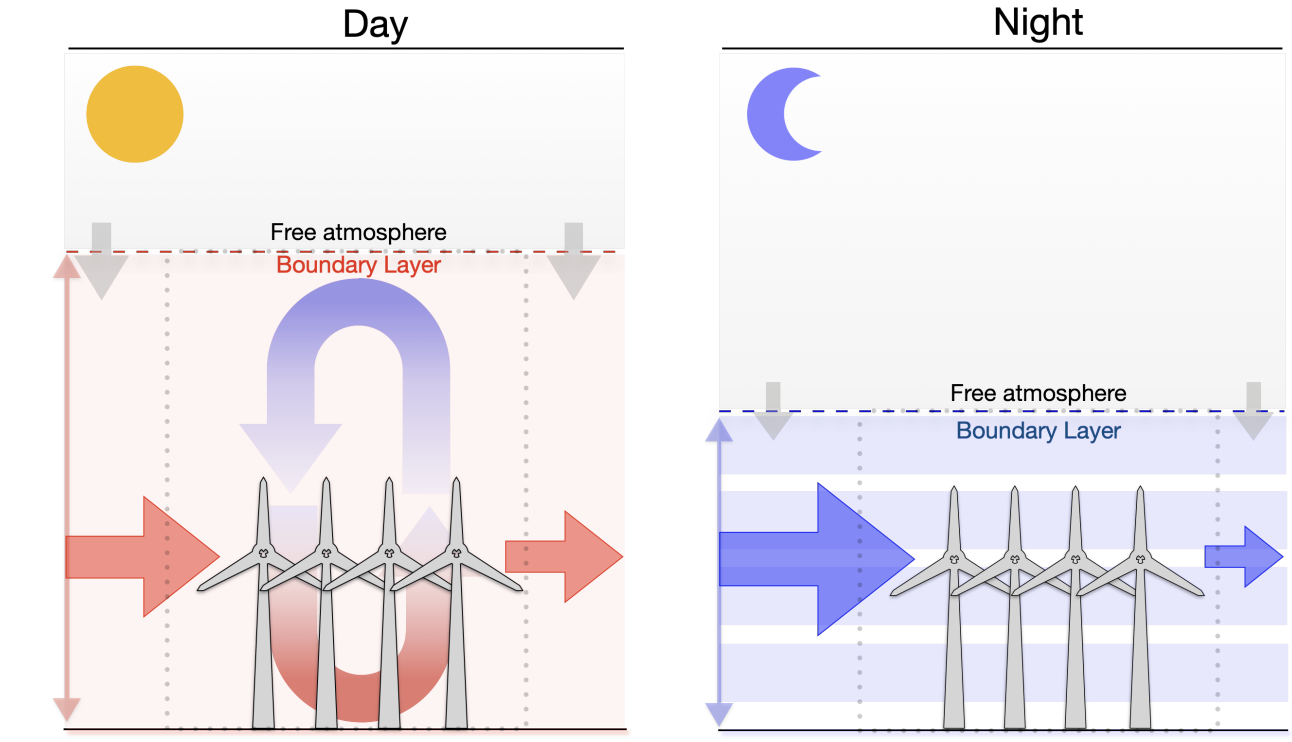

Figure 2. Differences between daytime (left) and nighttime (right) boundary layer conditions. Gray downward arrows represent the downward flux of kinetic energy from the free atmosphere into the boundary layer. The red and blue arrows represent the horizontal kinetic energy in- and outflow (from left to right) through the boundary layer volume bounding the regional scale wind turbine deployment (dotted box) during day and night, respectively. The free atmosphere represents the part of the atmosphere in which large-scale motion is generated in the absence of friction.

yields, despite higher incoming, undisturbed wind speeds. Thus, the differences in boundary layer characteristics during day and night will affect wind resource potentials of regional deployments of wind turbines.

Our goal in this paper is twofold: (1) to evaluate the effect just described to demonstrate the importance of a broader accounting of the atmosphere in technical potential estimation, and (2) to quantify the role of KE removal in shaping technical potentials at the regional scale. To accomplish our first goal, we will explicitly evaluate this difference between day and night by evaluating separate daytime and nighttime budgets in the KEBA approach. This is accomplished by prescribing different boundary layer heights in KEBA, which changes the size of the KE resource. Note that the effect of reduced turbulent mixing within the boundary layer is not accounted for. To accomplish our second goal, we use the scenarios of the previously published study for Kansas (Miller et al., 2015). We use the wind speeds of their control simulation without deployment to evaluate wind resource potentials using the standard approach as well as KEBA, and compare these to the estimates derived from the interactive model simulations.

https://doi.org/10.5194/wes-2023-82
Preprint. Discussion started: 10 November 2023

eawe european academy of wind energy
Open Access WIND ENERGY SCIENCE DISCUSSIONS

Table 1. Turbine characteristics of a Vestas V112 3 MW turbine, as in Miller et al. (2015).

Description	Symbol	Value	Units
Hub-height	H_{hub}	84	m
Rotor diameter	D	112	m
Rotor area	A_{rotor}	9852	m^2
Rated power	$P_{\text{el,max}}$	3.075	MW
Cut-in wind speed	v_{min}	3	m s^{-1}
Rated wind speed	v_{rated}	11.5	m^{-1}
Cut-out wind speed	v_{max}	25	m s^{-1}
Power coefficient (max.)	η_{max}	0.42	-

In the following section, we provide a brief description of the KE budget approach, the turbine deployment scenarios, and the model parameters used. We then present the KE budgets diagnosed from the simulations for the different scenarios, the reductions in wind speeds with greater wind energy use, and describe the effects on yield estimates and capacity factors. We also evaluate the importance of accounting for different boundary layer heights for the estimates. After a brief account of limitations, we then re-evaluate the wind resource potential and compare it to previously-published estimates (Lopez et al., 2012; Brown et al., 2016). We close with a discussion and conclusions.

2 Methods

We use the wind speeds, scenarios, and yield estimates from Miller et al.'s WRF simulations (Miller et al., 2015). We use these simulations as the reference in which the effects of wind turbines on the atmosphere are fully accounted for, and refer to the yield estimate as the "WRF" estimate. The simulations were performed with the WRF-ARW v3.3.1 regional weather research and forecasting model (Skamarock et al., 2008) to simulate different levels of hypothetical deployments of wind turbines over $112 \cdot 10^3$ km^2 in Kansas (Central US) using atmospheric conditions from May 15 to September 30, 2001. This period is considered to be climatologically representative for this region (Trier et al., 2010). The deployment area is similar to that assumed in previous resource evaluations (Lopez et al., 2012; Brown et al., 2016). Wind turbines are parameterized as elevated momentum sinks and sources of additional Turbulent Kinetic Energy (TKE) (Fitch et al., 2013b). The large, idealized deployments simulated a range of installed turbine capacity densities from 0.3125 to 100 MW km^{-2} which were equally distributed within the expansive wind farm area. Here we restrict the comparison to a maximum installed capacity density of 10 MW km^{-2}, yielding a total installed capacity of 35 GW to 1.1 TW over the region. The turbine characteristics and wind park scenarios, as well as the symbols used in the following, are summarized in Tables 1 and 2.

The "standard" and "KEBA" yield, or electricity, estimates were then calculated using hourly time series of wind speeds, v_{in}, from the WRF Control simulation, i.e., without any wind turbines present. The "standard" estimate replicates the standard approach used in existing policy side evaluations. It is based on the power curve of the turbine, the number of turbines in the

https://doi.org/10.5194/wes-2023-82
Preprint. Discussion started: 10 November 2023

eawe european academy of wind energy
Open Access WIND ENERGY SCIENCE DISCUSSIONS

Table 2. Scenarios of large-scale deployment of wind turbines in Kansas, Central US, evaluated here. Based on (Miller et al., 2015).

Description	Symbol	Value	Units
Width	W	$360 \cdot 10^3$	m
Length	L	$312 \cdot 10^3$	m
Capacity density	-	$0.3125 - 10$	MW km^{-2}
Number of turbines	N	11.7×10^3 - 3.7×10^5	-
Deployment area	A_{farm}	1.12×10^{11}	m^2

scenario, and the wind speeds, v_{in}. The electricity yield of the standard approach, $P_{\text{el,std}}$, is estimated from the turbine's power curve (Fig. 1b) by

$$P_{\text{el,std}} = N \cdot \min(P_{\text{el,max}}, \frac{\rho}{2} \cdot \eta_{\text{max}} \cdot A_{\text{rotor}} \cdot v_{\text{in}}^3) \tag{1}$$

where N is the number of turbines, $P_{\text{el,max}}$ is the rated capacity of the turbine, ρ is the air density (we used $\rho = 1.2$ kg m^{-3}), η_{max} is the maximum power coefficient, and A_{rotor} is the rotor-swept area, and v_{in} is the wind speed from the WRF Control simulation (Table 1). This estimate assumes that the effects of the KE removal by the wind turbines is fully compensated for by the inter-turbine spacing, which allows wind speeds and capacity factors to be unaffected by presence of a wind turbine deployment in the region.

The "KEBA" estimate is derived from the KEBA model (Kleidon and Miller, 2020) augmented with information about day- and nighttime boundary layer heights derived from the WRF simulations. The budgeting of the KE fluxes of the boundary layer over the deployment region results in a reduction factor f_{red}. This factor encapsulates the effect of KE removal from the wind by the turbines on wind speeds and turbine yields. In KEBA, the wake loss term is fixed as half of the deployment yield after the work of Corten(Corten, 2001). First, f_{red} is applied to the WRF control wind speeds (v_{in}) to quantify the reduction in the wind speeds (v_{eff}).

$$v_{\text{eff}} = f_{\text{red}}^{\frac{1}{3}} \cdot v_{\text{in}} \tag{2}$$

Then, v_{eff} is applied to the standard estimate (Equation 1) instead of v_{in} to derive the KEBA estimate of deployment yields ($P_{\text{el,keba}}$). This results in the following expression for deployment yield (see Kleidon and Miller (2020) for detailed derivation)

$$P_{\text{el,keba}} = N \cdot \min(P_{\text{el,max}}, f_{\text{red}} \cdot \frac{\rho}{2} \cdot \eta_{\text{max}} \cdot A_{\text{rotor}} \cdot v_{\text{in}}^3) \tag{3}$$

The reduction factor f_{red} is represented by

$$f_{\text{red}} = \frac{H + 2C_d \cdot L}{H + 2C_d \cdot L + \frac{3}{2} \cdot \frac{N}{W} \cdot \eta_{\text{max}} \cdot A_{\text{rotor}}} \tag{4}$$

https://doi.org/10.5194/wes-2023-82
Preprint. Discussion started: 10 November 2023

eawe european academy of wind energy
Open Access WIND ENERGY SCIENCE DISCUSSIONS

for wind speeds v_{in} above the cut-in velocity v_{min} and below the rated velocity v_{rated} when the turbine output is proportional to the incoming wind speeds (2b); and

$$f_{\text{red}} = 1 - \frac{3}{2} \cdot \frac{1}{H + 2C_d \cdot L} \cdot \frac{H}{L} \cdot \frac{N \cdot P_{el,max}}{J_{in,h}} \tag{5}$$

for v_{in} greater than the rated velocity v_{rated}, but below the cut-out velocity, v_{max}. For this case, f_{red} is computed only to simulate the effect of wind speed reduction for comparison. Note that the case of $f_{\text{red}} = 1$, KEBA represents the standard approach.

In these equations for f_{red}, H is the height of the boundary layer (Table 3), C_d is the aerodynamic drag coefficient of the surface (Table 3), L and W the length and width of the deployment (Table 2), and $J_{\text{in,h}}$ the horizontal kinetic energy flux in the boundary layer ($\rho/2 \cdot v_{\text{in}}^3 \cdot WH$). The values for daytime and nighttime mean boundary layer heights are provided in Table 3. They were derived by comparison of the vertical velocity profiles of the WRF simulations with and without the wind turbine deployment, yielding mean values of about 2000m (day) and 900m (night) (see Appendix A).

The kinetic energy budgets for the different scenarios are diagnosed from the time series of the velocity v_{in} and f_{red} and then averaged, with the different terms estimated as in Kleidon and Miller (Kleidon and Miller, 2020). The budget is defined for the boundary layer air volume enclosing the deployment of wind turbines, given by the dimensions W and L (Table 2), as well as the height of the boundary layer H (Table 3). The magnitude of the budget is set by the influx of kinetic energy, which is determined by the horizontal ($J_{\text{in,h}} = WH \cdot \frac{\rho}{2} v_{\text{in}}^3$) and vertical ($J_{\text{in,v}} = WL \cdot \rho C_d v_{\text{in}}^3$) influxes of kinetic energy into the volume. This energy is then either dissipated by surface friction, used for electricity generation, dissipated by wake turbulence, or exported downwind.

Table 3. Atmospheric and environmental specifications needed for the KEBA estimate.

Description	Symbol	Value	Units	Comments
Boundary layer height-Day	H_{day}	2000	m	Mean, fixed
Boundary layer height-Night	H_{night}	900	m	Mean, fixed
Drag coefficient	C_{d}	0.001	-	Mean, fixed

3 Results & Discussion

We posited that the KE budget is central to capturing the reduction in wind speeds with increased installed capacity to understand the difference between daytime and nighttime yields as shown in Fig. 1, and quantifying the resulting technical potential. Therefore, we start by showing the KE budgets during day and night for the different scenarios, the regional reduction in wind speeds, before we describe the estimated yields and capacity factors. We then perform a sensitivity analysis to boundary layer height to evaluate the effects of the day-night differences and compare these to the general effect of reduced wind speeds with

https://doi.org/10.5194/wes-2023-82
Preprint. Discussion started: 10 November 2023

eawe european academy of wind energy
Open Access WIND ENERGY SCIENCE DISCUSSIONS

greater installed capacities. We end this section with a discussion on the limitations, the resulting resource potential estimate, and the broader implications.

3.1 Kinetic Energy budgets

The KE budget of the boundary layer volume enclosing the deployment is central to KEBA estimates, with the magnitude of the budget defining the wind speed reductions and limiting deployment yields. The horizontal influx accounts for a larger share of the KE budget than the vertical input: 76% during daytime and 60% during nighttime. The combination of lower daytime wind speeds ($v_{\text{day,mean}}$ = 6.8 $m\,s^{-1}$) and higher boundary heights (H_{day} = 2000m) and higher nighttime wind speeds ($v_{\text{night,mean}}$ = 9.5 m s^{-1}) and lower boundary layer heights (H_{night} = 900m) lead to similar influxes of kinetic energy of about 150 GW in the mean. The 150 GW budget sets the overall magnitude of the bars in Fig. 3(a), with the distribution among the different terms changing due to the different deployment scenarios.

Within the boundary layer volume, KEBA determines the partitioning between the KE influx into frictional dissipation (red), wind turbine yields (dark blue) and wake losses (light blue), and the downwind export of KE out of the deployment volume (light red). KE extracted by wind turbines powers electricity generation ($P_{\text{el,tot}}$), with the wakes being dissipated by the mixing behind the turbines (D_{wake}). KE extraction consumes KE that would have otherwise been dissipated at the surface by friction or exported downwind. Thus, the increase in capacity density increases yields and wake losses at the expense of KE in downwind export and surface friction. Since individual turbine yields depend on wind speeds, higher nighttime mean wind speeds lead to higher per turbine yield compared to the daytime. Consequently, about 2% more KE is extracted by the turbines from the budget at night than during the day (Fig. 3(a)).

3.2 Wind speeds

The depletion of the KE budget with increased wind turbine deployment is associated with a reduction in wind speeds. This reduction is shown in Fig. 3(b), which shows how the mean wind speed over the deployment region (v_{eff}) reduces with the amount of KE extracted by the wind turbines (in W m^{-2} of surface area). We chose to use the yield on the x-axis rather than installed capacity, because in this way, it shows that wind speed reductions are almost linear with the amount of KE extracted. Figure 3(b) shows these wind speed reductions for the WRF estimate (red) and the KEBA estimate (blue), while the standard approach (grey) assumes no change in wind speeds. The rates of reduction can be quantified by the slope, m, of the linear regressions (dashed lines). Nighttime wind speed reductions ($m_{\text{KEBA,night}} = -6.21$) are almost twice as strong as during the day ($m_{\text{KEBA,day}} = -3.89$). These reduction rates are similar in the WRF estimates ($m_{\text{wrf,night}} = -10.53, m_{\text{wrf,day}} = -3.15$). Note that despite the faster rate of reduction in nighttime means, the wind speeds are nevertheless higher in magnitude than during the daytime. Compared to the WRF simulations, KEBA slightly overestimates daytime and underestimates nighttime wind speeds. Thus, the difference in daytime and nighttime wind speed reductions can be directly linked to the lower boundary layer height used in the nighttime KE budget in KEBA.

https://doi.org/10.5194/wes-2023-82
Preprint. Discussion started: 10 November 2023

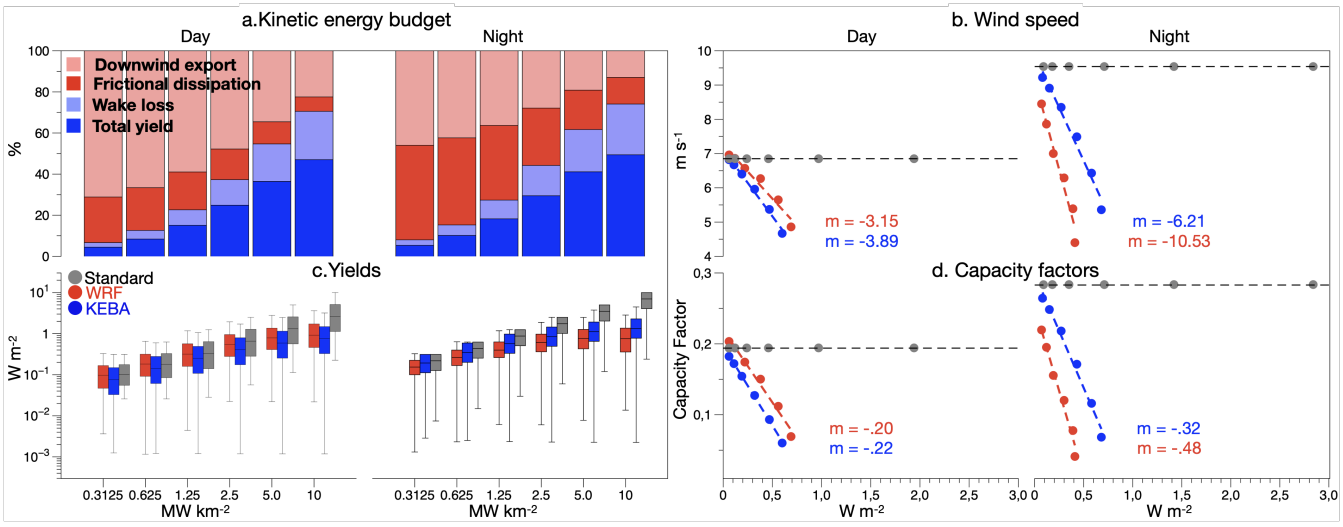

Figure 3. (a) Daytime (left) and nighttime (right) KE budgets, with total yields (dark blue), wake loss (light blue), frictional dissipation (red) and the downwind export (light red). (b) Estimates of wind speeds over the deployment region against the KE extracted by the wind turbines for the "standard" (grey), "WRF" (red) and "KEBA" (blue) estimates. (c) Wind turbine yields as a function of installed capacity density using a logarithmic scale for the “standard" (grey), "WRF" (red) and "KEBA" (blue) estimates. (d) Capacity factors against the rate of KE extraction for the "standard" (grey), "WRF" (red) and "KEBA" (blue) estimates. Dashed lines denote linear fits, with m values providing the slopes obtained from the linear regression.

3.3 Deployment yields

Figure 3(c) shows the variation in the wind turbine yields with increasing installed capacity density. Since KEBA models yields as a function of the reduced wind speeds (v_{eff}) rather than the prescribed Control wind speeds (v_{in}), its estimates (blue) are lower than the standard estimates (gray). KEBA estimates lower additional increments in yields with the increase in installed capacity during both, day and night. Thus, the diminishing increments in yields with added turbines can be attributed directly to the reduced wind speeds shown in Fig. 3(b). While KEBA estimates of nighttime yields are higher than day, WRF estimates of yield (red) are lower at night than during the day. KEBA captures the trends in yields increments but does not estimate the lower-than-daytime yields at night. It underestimates WRF’s mean daytime estimates by 8 - 15% while overestimating nighttime yields by 20 to 75%. The standard estimate overestimates yields by up to 180% during daytime and up to 600% at night compared to the WRF estimates. The bias in KEBA estimates of yield compared to WRF can be attributed to higher nighttime KEBA wind speed estimates.

3.4 Capacity Factors

The lower increments in yields with increased installed capacity indicates that more turbines within the deployment region lowers the mean efficiency of individual turbines. This can be shown by directly looking at the capacity factors, as displayed

https://doi.org/10.5194/wes-2023-82
Preprint. Discussion started: 10 November 2023

eawe european academy of wind energy
Open Access WIND ENERGY SCIENCE DISCUSSIONS

in Fig. 3(d). Both, KEBA (blue) and WRF (red) estimates show that increasing KE extraction leads to lower capacity factors. The standard estimate (grey), however, assumes no change because no reduction in wind speeds is considered. Again, as in the case for wind speeds, the capacity factors reduce almost linearly with increasing KE extraction. The slopes of the linear regression show that turbine efficiencies reduce almost twice as fast during the night ($m_{\text{KEBA,night}} = -.32$) than during the day ($m_{\text{KEBA,day}} = -.22$), which is similar to the WRF estimates ($m_{\text{wrf,night}} = -.48$) and ($m_{\text{wrf,day}} = -.20$). While KEBA, again, underestimates the strength of the reduction at night, the close match of KEBA estimates with the WRF estimates highlights that the removal of KE from the boundary layer is the main effect that results in reduced turbine efficiencies and wind turbine yields. KEBA is able to capture a large part of this trend because of the separate definition of day and night KE budgets as opposed to a single KE budget for the whole day.

3.5 Role of diurnal variations in boundary layer height

To evaluate how important the variation in boundary layer height is for estimating yields between day and night, we performed an additional estimate with KEBA in which the boundary layer height is fixed to the mean value of $H = 1268$m (as in Miller et al. (2015)). This comparison is shown in Fig. 4. Although the KEBA estimate with a single mean boundary layer height represents a substantial improvement over the standard estimate, it shows a greater discrepancy to the WRF estimate. Nighttime yields are overestimated by 20 to 107% while daytime yields are underestimated by 12 to 31%. The addition of diurnal variations in boundary layer height improves the estimates relative to WRF estimate, reducing the daytime bias to 10 to 17% and nighttime bias to 20 to 60%. The improvement is more pronounced for the nighttime conditions.

Defining different day and nighttime budgets separately is thus an improvement over neglecting this variation. It captures more of the underlying mechanism because the daytime solar insolation drives convective motion and higher mean boundary layer heights. The absence of these motions at night lead to much lower boundary layer heights. The difference in the amount of mixing between day and night differentially affects the wind speeds and deployment yields during day and night (Fitch et al., 2013a; Abkar et al., 2016). With all other variables in the KEBA model being fixed, a fixed boundary layer height in KEBA results in a 58% lower daytime and 30% higher nighttime KE budget compared to a variable boundary layer height. Although the bias is not entirely compensated for by including the varying boundary layer heights in the KEBA estimates, this information clearly reduces the bias in the direction of the WRF estimate. However, the effect of these diurnal variations at the daily 24 hour scale is relatively muted. This is because the higher day and lower nighttime generations largely compensate for each other implying that it is mainly the role of KE removal that needs to be incorporated in the policy focused estimation of technical potentials.

3.6 Limitations

Although KEBA captures day and night trends produced by WRF better than the standard approach, it is unable to reproduce the lower-than-day, nighttime wind turbine yields from WRF. This is likely because KEBA assumes a well-mixed boundary layer volume that is characterized by one effective wind speed, v_{eff}. This assumption is valid during the day when the convective boundary layer is well mixed. At night, however, stable conditions prevent vertical mixing because the insolation-driven

https://doi.org/10.5194/wes-2023-82
Preprint. Discussion started: 10 November 2023

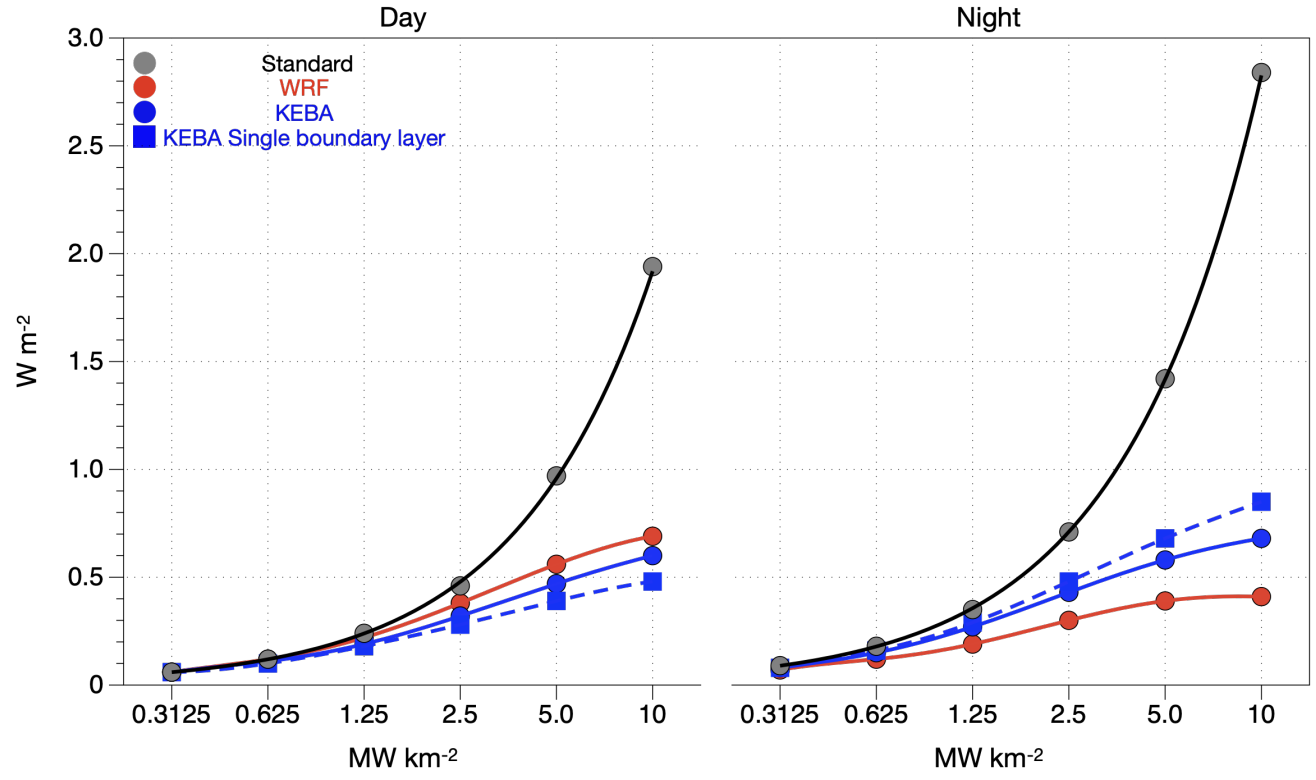

Figure 4. Daytime (left) and nighttime (right) total yields estimated by WRF (red ◯), KEBA with (blue ◯) and without (blue □) diurnal variations in boundary layer height, and the standard approach (grey ◯).

convective motions are absent. The intensity of mixing within the boundary layer is thus an additional control on the rate at which the KE deficit behind wind turbines is replenished within the boundary layer. The less-mixed nighttime boundary layer slows the replenishment rate, leading to a steeper decline in wind speeds, capacity factors and wind turbine yields (Fitch et al., 2013a; Abkar et al., 2016).

This interpretation is supported by observations of velocity deficits, or wakes, behind operating offshore wind farms that persist longer when the vertical mixing is lower (55km) than when it is higher (35km)(Cañadillas et al., 2020; Christiansen and Hasager, 2005). Longer wakes during less mixed conditions imply lower downward replenishment than better mixed conditions, leading to slower recovery of wind speeds.

Reported simulated day- and nighttime mean wind speed reductions of 10 and 30% (Fitch et al., 2013a) from Kansas are similar to the estimates of Miller et al. of 17% and 43%. WRF estimates for wind turbine yields during day (42% lower than standard) and night (73%) are consistent with other simulations of idealized deployment yields over a full diurnal cycle which found that reductions were twice as high at night (57%) than daytime (28%)(Abkar et al., 2016). Thus, it is likely that the

https://doi.org/10.5194/wes-2023-82
Preprint. Discussion started: 10 November 2023

eawe european academy of wind energy
Open Access WIND ENERGY SCIENCE DISCUSSIONS

differences between WRF and KEBA could be reduced by accounting for stability effects, which could be taken up as a part of future work.

Despite this limitation, KEBA represents a significant improvement over the standard approach, especially with greater installed capacities over the region. Its nighttime yield estimates are within a factor of 2 of the WRF estimate. The standard approach overestimates WRF yields by up to 6 times. Our results highlight the critical role of boundary layer information, in terms of height and mixing/stability, in determining KE budgets that shape the extent to which wind speeds, turbine efficiencies and deployment yields are affected by the removal of KE. Thus, the KEBA estimate appears to be a suitable tool to evaluate Kansas's technical wind energy potential.

3.7 Reevaluating Kansas's technical potential

Table 4. Comparison of previously published estimates of the technical wind energy potential of Kansas by (Lopez et al., 2012; Brown et al., 2016) with the estimates from this study. For the comparison, we used the scenarios with installed capacity densities of 2.5 and 5 MW km^{-2}, which are close to these previous estimates. A 15% array efficiency reduction was applied to the Standard estimate.

Lopez et al. (2012)		Standard	KEBA	WRF
Deployment area (km^2)	190 000			
Capacity density (MW km^{-2})	5	5	5	5
Capacity factor (%)	37	41	21	19
Yield (W m^{-2})	1.86	2.03	1.05	0.95
Technical potential (TWh yr^{-1})	3101	3379	1748	1581
Difference (%)		+9.0	-43.6	-49.0
Brown et al. (2016)		Standard	KEBA	WRF
Deployment area (km^2)	157 890			
Capacity density (MW km^{-2})	3	2.5	2.5	2.5
Capacity factor (%)	45	41	31	27
Yield (W m^{-2})	1.36	1.02	0.75	0.68
Technical potential (TWh yr^{-1})	1877	1410	1037	941
Difference (%)		-24.9	-44.8	-49.9

To illustrate the relevance of these KE removal effects, we compare our estimates to the existing technical potentials for Kansas (Lopez et al., 2012; Brown et al., 2016). This comparison is summarised in Table 4. Previous studies estimate potentials of 3101 TWh yr^{-1} and 1877 TWh yr^{-1} for capacity densities of 5 and 3 MW km^{-2} over $1.9 \cdot 10^5$ km^2 and $1.6 \cdot 10^5$ km^2, respectively, which include a fixed, 15% loss in array efficiency. This results in capacity factors of 37% and 45%. Expressed in terms of yields, these estimates imply 1.86 W m^{-2} and 1.36 W m^{-2} of generated electricity per unit surface area. Multiplied by the deployment areas, these yield technical potentials of 3101 TWh/a and 1877 TWh/a for Kansas in these previous studies.

https://doi.org/10.5194/wes-2023-82
Preprint. Discussion started: 10 November 2023

eawe european academy of wind energy
Open Access WIND ENERGY SCIENCE DISCUSSIONS

We first compare our standard estimate to these resource estimates, using our scenarios with installed capacity densities of 5 and 2.5 MW km^{-2}. For these scenarios, the yield is on average 2.39 W m^{-2} and 1.19 W m^{-2}, with a capacity factor of 48%. We reduce these estimates by the same 15% loss, which reduces the yields to 2.03 W m^{-2} and 1.02 W m^{-2} with a 41% capacity factor. Multiplied by the deployment areas, these yield technical potentials of 3379 TWh/a and 1410 TWh/a, which are within $\pm$25% of the published estimates.

KEBA estimates lower yields of 1.05 W m^{-2} and 0.75 W m^{-2} for the two scenarios, with capacity factors reduced to 21% and 31%, respectively. These reductions compare well with the WRF estimates of 0.95 and 0.68 W m^{-2} and capacity factors of 19% and 27% from Miller et al.. Multiplied by the deployment areas, these yield technical potentials of 1748 TWh/a and 1037 TWh/a using KEBA, and 1581 TWh/a and 941 TWh/a using WRF. These estimates for the technical potentials are lower by 40-50% due to the reductions in wind speeds.

Wind speed reductions are thus likely to play a substantial role in lowering regional-scale technical resource potentials than those that use prescribed wind speeds. Note that the potential is nevertheless 3 to 5 times the total energy consumed by the state in 2018 (kan (2018)).

3.8 Implications for technical wind energy potential estimation

The reduced technical potentials derived using KEBA are consistent with previous climate (GCM) and weather modelling (WRF) estimates. This is shown in Fig. 5 in which the variation of technical potential in Kansas is plotted against the capacity density deployed. KEBA estimates are represented in blue, standard estimates in black and numerical estimates are shown in red. Broadly, the black colour represents the exclusion of KE removal effects while blue and red represent partial (KEBA) and complete inclusion (WRF and GCM), respectively. The stars represent results from this study while the black square (Lopez et al., 2012) and circle (Brown et al., 2016) represent previously published estimates of Kansas's potential. The black dotted lines represent the variation in potential linked to the standard estimates from this study (black stars (Miller et al., 2015)). The red stars (Miller et al., 2015) and pentagons (Volker et al., 2017) represent previous WRF-based estimates of Kansas. The dotted red line shows the peak average potential from large deployments in Central USA as estimated by Adams and Keith (Adams and Keith, 2013). Similarly, the red circles (Jacobson and Archer, 2012) and squares (Miller and Kleidon, 2016) represent the trends over global land (26% of global area) derived using GCMs. The blue band highlights the range of peak average global potentials estimated previously (Miller et al., 2011; Jacobson and Archer, 2012; Miller and Kleidon, 2016; Marvel et al., 2012; Wang and Prinn, 2010, 2011; Gustavson, 1979). The red circle with a blue outline represents an observations - based study of generation from currently operating onshore wind farms in the Central US(Miller and Keith, 2018). Numerical estimates in Kansas show that beyond 1.5 MW km^{-2} of deployed capacity in Kansas leads to 50% lower potential (red) compared to the standard estimates. Even though potential increases with increasing capacity deployment, it is not linear as implied by the standard estimates. This sub-linear increase with installed capacity shows that capacity factors reduce with the increasing deployment. All the numerically simulated estimates display similar variation in potential with capacity and culminate near an average peak of 1.1 W m^{-2}. This variation is also consistent with global estimates over land, albeit higher, because Kansas is winder than most places(Miller et al., 2015). In line with these estimates, Miller and Keith (Miller and Keith, 2018) showed

https://doi.org/10.5194/wes-2023-82
Preprint. Discussion started: 10 November 2023

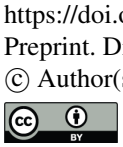

eawe european academy of wind energy
Open Access WIND ENERGY SCIENCE DISCUSSIONS

that the actual yield from an average estimated onshore US capacity density of 2.7 MW km^{-2} is around 0.90 W m^{-2}. The agreement between estimates from independent numerical modelling studies and relevant observational data analysis points to the robustness of this trend. The variation in KEBA estimates (blue) is consistent with these trends. Although the match between KEBA and the numerical estimates is not exact, it highlights the significance of the effects of KE removal effects on technical potential.

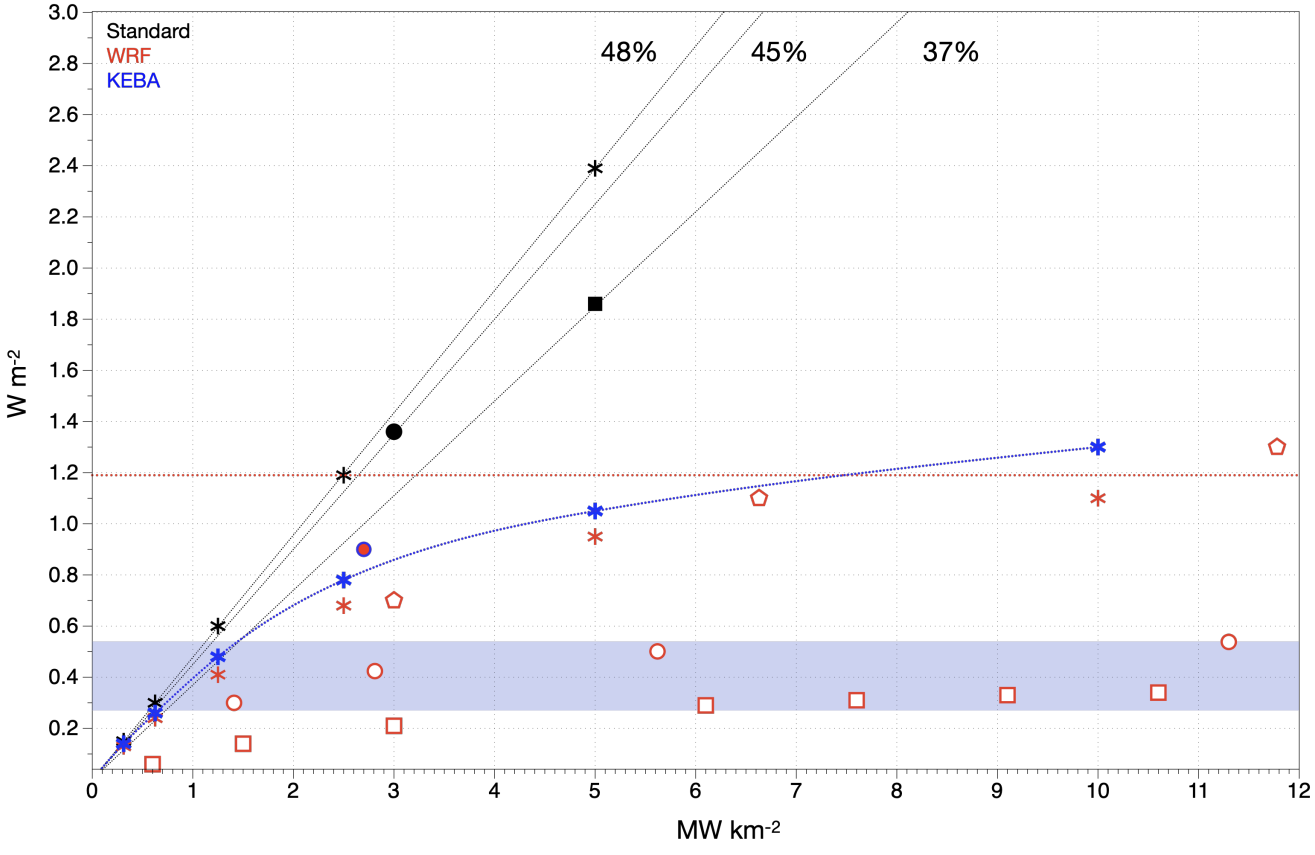

Figure 5. Technical potentials per unit surface area plotted against the capacity density and number of turbines (x-axis). Black symbols represent standard estimates (No KE removal), while red symbols represent meteorological estimates (With KE removal). Blue symbols represent the KEBA estimates from this study. The blue band represents the range of average peak global potentials (Miller et al., 2011; Jacobson and Archer, 2012; Miller and Kleidon, 2016; Marvel et al., 2012; Wang and Prinn, 2010, 2011; Gustavson, 1979). The red dotted line represents the peak average potential of Kansas (Adams and Keith, 2013) while the dotted lines show the assumed capacity factors without accounting for the removal of KE. Existing estimates of the Kansas resource potential are shown in black filled symbols(Brown et al., 2016; Lopez et al., 2012).The red circle with the blue outline shows an observation-based estimate (Miller and Keith, 2018)

The comparison in Fig. 5 shows that the removal of KE is the predominant physical influence which shapes the technical potential of Kansas. The close agreement between KEBA, which only accounts for KE removal effects, and the WRF trends,

https://doi.org/10.5194/wes-2023-82
Preprint. Discussion started: 10 November 2023

eawe european academy of wind energy
Open Access WIND ENERGY SCIENCE DISCUSSIONS

which includes effects arising from both KE removal and stability, highlights the the role of the KE removal as the predominant influence on technical potentials. The remaining difference indicates the secondary role of stability or the degree of mixing in the boundary layer.

Including just the KE removal effect leads to a significant improvement in estimates over the standard estimates. Although diurnal variations in stability lead to variations in wind speeds reductions, yields and capacity factors during day and night, the effect of these on the estimated technical potential is marginal over the whole time period. Including additional boundary layer information into KEBA improves the agreement during day and night time but is unable to completely capture stability effects.

Nevertheless, KEBA still provides a straightforward physical framework through which the role of different physical influences on the resource potential, in this case diurnal variations, can be better understood and quantified.

The reduced technical potentials and capacity factors significantly affect the economic potential of wind energy. This is commonly considered by evaluating the economic cost of wind energy using the Levelised Cost of Energy (LCOE) (Ragheb, 2017; Blanco, 2009). We use the estimates from above and plot these in terms of a relative increase in the LCOE in Fig. 6.

In the standard approach, based on its assumption of constant wind speeds, standard capacity factors remain constant while technical potential increases linearly. A doubling of capacity leads to a doubling of the potential. To estimate LCOE based on standard estimates, we assume that cost of wind energy is only a function of the number of turbines. Then, the LCOE becomes an inverse function of the capacity (see supplementary materials for details). Thus, there is no change in the standard LCOE as capacity factors remain unchanged (gray stippled line).

In the case of WRF (red circles) and KEBA (blue squares), however, technical potentials increase sub-linearly (Fig. 6a) and the capacity factors reduce (Fig. 6b). Each doubling of turbines from the lowest scenario to the 2.5 MW km^{-2} scenario leads to an average of 70 - 75% stepwise increments in potential coupled with an average of 11 - 14% stepwise reduction in capacity factors. Each doubling in capacity beyond this leads to average stepwise increment of 27 - 31% in potential coupled with average reductions in capacity factors of 35 - 40%. Since we assumed that LCOE is only inversely related to capacity factor, reductions in them lead to increases in LCOE, relative to the standard LCOE estimate. Thus, KEBA and WRF lead to estimates of LCOE that are on average 80 - 120% higher than the standard estimates at an installed capacity density of 5 MW km^{-2}.

This increase in LCOE due to KE removal remains unaccounted for in policy evaluation because the effect of KE removal on technical potentials and capacity factors is implicitly neglected in the standard approach(Wiser et al., 2016). It should be noted that although we present a simplified illustration, even a detailed LCOE calculation is likely to show similar trends given that LCOE values are highly sensitive to variations in capacity factors (Blanco, 2009). Thus, the reduced potentials arising from KE removal have a significant impact on LCOE which need to be explicitly evaluated in policy evaluations.

4 Conclusions

We conclude that the KE removal effect is the predominant physical influence that shapes technical wind resource potentials at the regional scale. Although day- and nighttime boundary layer heights and stability conditions affect the technical potential, it

https://doi.org/10.5194/wes-2023-82
Preprint. Discussion started: 10 November 2023

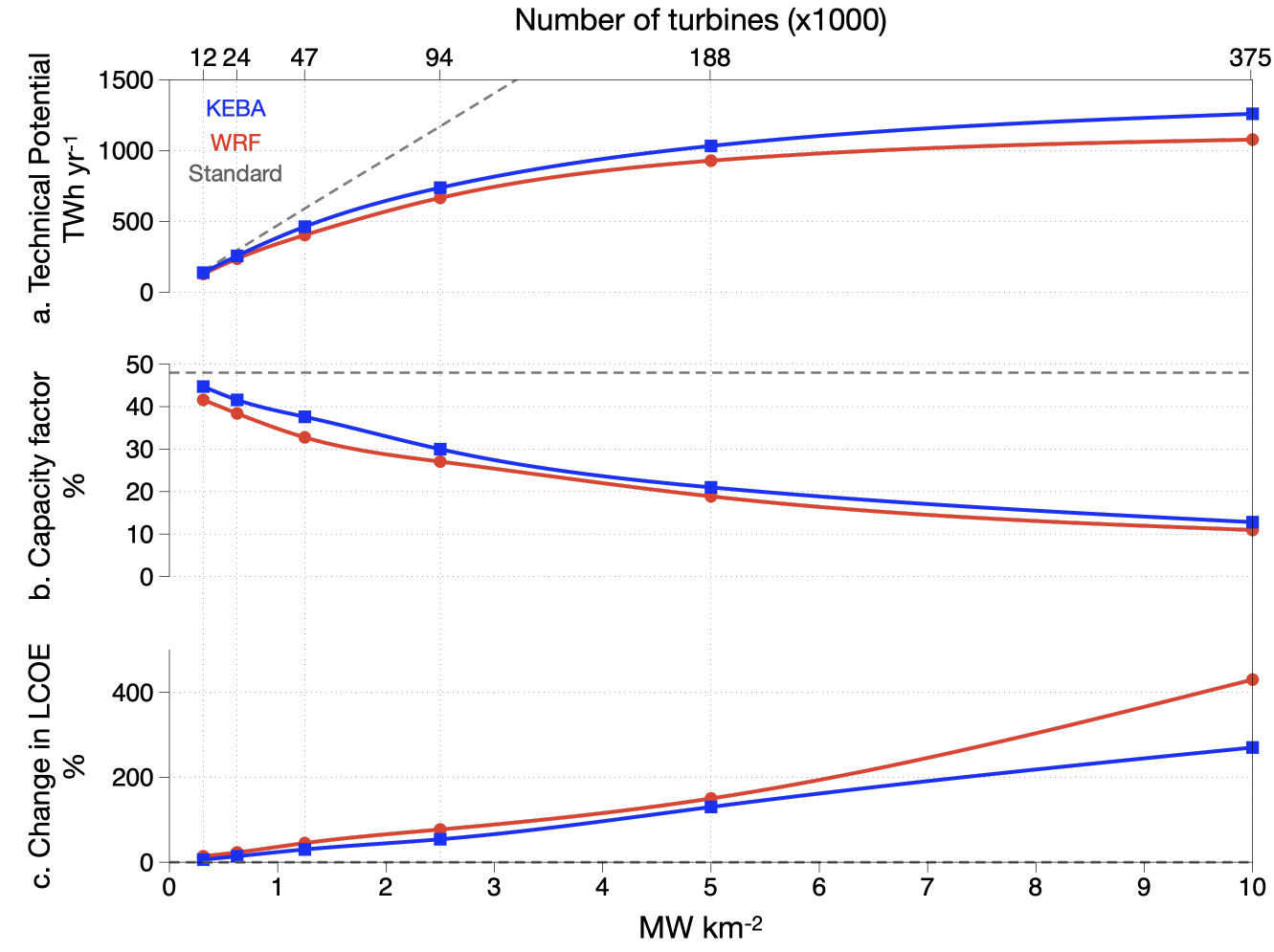

Figure 6. (a.) Variation in WRF(red ◯) KEBA (blue □) and standard (gray stippled lines) estimates of technical potential,(b.) capacity factors, and (c.) % change in the Levelised Cost of Energy (LCOE) relative to the standard LCOE estimate plotted as a function of capacity densities (bottom) and number of turbines deployed (top).

is the removal of KE from the wind that, primarily, shapes the reduction in wind speeds and capacity factors. It leads to reduced potentials compared to the standard approach that have a significant impact on the economic potential of wind energy at larger scales.

These impacts need to be assessed in policy evaluations of wind energy and the energy transition. For this KEBA is a viable alternative to the standard approach because it is simple to implement (Kleidon and Miller, 2020) and accounts for the effect of the key atmospheric control on technical potentials. This is not to negate the use of more physically comprehensive, numerical methods like WRF and GCMs in policy analyses but to enable energy scenario modellers without a background in

https://doi.org/10.5194/wes-2023-82
Preprint. Discussion started: 10 November 2023

eawe european academy of wind energy
Open Access WIND ENERGY SCIENCE DISCUSSIONS

meteorology to be able to incorporate the key physics without significantly increasing their models' computational complexity. The heavy computational requirements associated with physically accurate descriptions of the atmospheric circulations have been reported to inhibit their widespread incorporation into policy side evaluations (Staffell and Pfenninger, 2016).

Lastly, despite these detrimental effects at larger deployment scales, KEBA's estimates agree with previous research that has shown that wind energy is an abundant and renewable resource that can be harvested to meet a significant part of the future energy demand through efficient, large scale deployment of wind turbines (Jacobson and Archer, 2012; Volker et al., 2017).

Code and data availability. Code and data related to this analysis is available through Max Planck Society's Open Research Data Repository(EDMOND). The associated doi is : https://doi.org/10.17617/3.78

Appendix A

A1 Determining boundary layer heights for initialising KEBA

The KEBA model estimates park yield and mean wind speed reduction through the application of conservation of energy ((Kleidon and Miller, 2020)). The kinetic energy (KE) generated in the atmospheric boundary layer is balanced by that consumed by the wind turbines within the wind park and its wake, dissipated at the surface, and that which powers the remnant wind. The KE conservation is applied to a hypothetical boundary layer volume which encompasses the wind turbine deployment and is mathematically represented as $J_{in,v} + J_{in,h} = P_{el,keba} + P_{wake} + D_{surface} + J_{out,h}$.The left hand side of this equation describes the horizontal and vertical flux of KE in to the boundary layer volume while the right hand side describes how this is partitioned within the volume. The vertical and horizontal KE fluxes into the volume can be expanded in to $J_{in,v} = WL \cdot \rho C_d \cdot v_{in}^3$ and $J_{in,h} = WH.\frac{\rho}{2} \cdot v_{in}^3$.

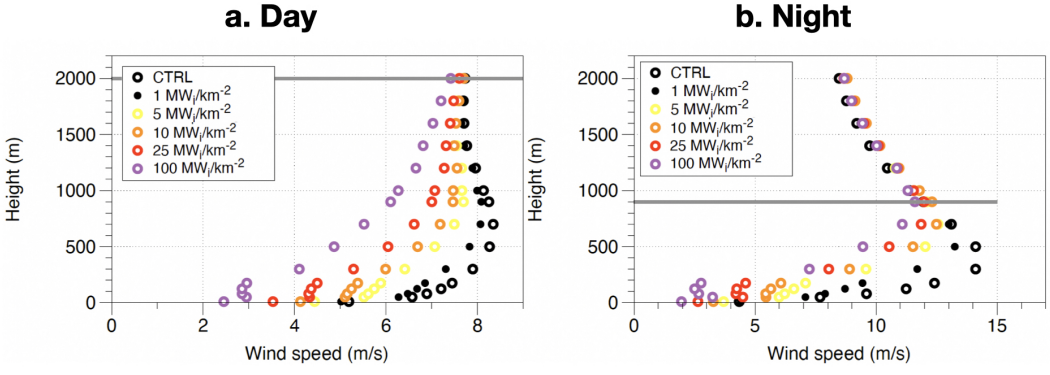

Figure A1. Day and night time wind vertical wind speed profiles estimated by Miller et al. (2015) which show that mean day-time boundary layer height is 2000m whereas that at night is 900m

https://doi.org/10.5194/wes-2023-82
Preprint. Discussion started: 10 November 2023

eawe european academy of wind energy
Open Access WIND ENERGY SCIENCE DISCUSSIONS

These expressions show that the KE budget available to the wind turbine deployment, is dependent on its geometry (cross-wind width W and downwind length L) and the height of the atmospheric boundary layer(H). In our analysis, the geometry of the deployment is fixed, therefore the only control on the KE budget is the boundary layer height. Changes in boundary layer height affect the horizontal input of KE flux ($J_{in,h}$). In line with the general definition of the atmospheric boundary layer as the layer which responds quickly to changes in surface forcing (Stull (2009)), the boundary layer from a KE perspective can be also defined as a layer, the kinetic energy content of which responds to changes in surface forcing i.e presence of large wind turbine deployments. Then the boundary layer height can be understood as the maximum height, up-till which the effects of kinetic energy removal by the turbines can be observed. Since the extraction of KE reduces mean wind speeds, changes in mean wind speeds induced by the turbines can be used estimate this height.

The mean wind speeds over the region of interest, Kansas in this case, were extracted by Miller et al. (2015) from their WRF simulations. Mean wind speeds were estimated per vertical model level over Kansas for the time period of simulation. Such mean wind speed estimates were computed for all WRF simulations i.e those without wind parks (CTRL) and those with ($0.3125 - 100 MW_i \cdot km^{-2}$). These mean wind speeds from the different models when plotted against model height (m) highlight the vertical variation of mean wind speeds or the vertical wind speed profiles. These are plotted for day and night separately in Fig. A1. In both the plots, the vertical wind speed profiles for the CTRL simulation represent the background circulation in the absence of any wind turbines and hence represent the undisturbed circulation. Vertical wind speed profiles for other simulations deviate from the CTRL trend because turbines extract KE from the wind speeds, thus slowing them down. The larger the number of turbines within the wind park, the greater is the deviation from the CTRL or the undisturbed trend. The mean day and night boundary layer heights for initialising the KEBA model are then those at which the vertical profiles derived from simulations with wind parks realign themselves with the undisturbed trend. Using this approach Miller et al 2015, estimated the day-time boundary layer height to be 2000m and the night-time boundary layer height to be 900m.

A1 Wind speed reductions

Here we tabulate (Table S1) the mean wind speed data simulated by Miller et al. (2015) without any wind parks or control (CTRL), and with the impact of wind parks with a range of turbine densities ($0.3125 - 10 MW_i\, km^{-2}$) split by day and night. Along with it we also provide the mean wind speed reductions estimated by KEBA with different day and night mean boundary layer heights.

A1 Park yield and capacity factors

This section contains tables containing information about park yields and capacity factors estimated by Miller et al. (2015) (WRF) and by us using the standard approach and the 2 different implementations of KEBA i.e with a single boundary layer height (KEBA single) and another with 2 different average heights (KEBA variable) for day (2000m) and night(900m) for all the capacity density scenarios simulated considered in (0.3125 - 10 MW km^{-2}). Tables S2 and S3 contain the data split between day and night time, respectively, whereas Table S4 contains the undifferentiated data.

https://doi.org/10.5194/wes-2023-82
Preprint. Discussion started: 10 November 2023

eawe european academy of wind energy
Open Access WIND ENERGY SCIENCE DISCUSSIONS

Table A1. This table contains shows wind speed predictions by WRF and KEBA split by day and night. The column titled "standard" represents the CTRL wind speeds i.e with out the impact of reduced wind speeds. Since the standard approach predicts no change to mean wind speeds despite removal of kinetic energy. Thus day and night winds speeds remain constant and same as the CTRL wind speeds.

Capacity Density	Standard Day	WRF Day	KEBA Day	Standard Night	WRF Night	KEBA Night
$MW_i\,km^{-2}$	$m\,s^{-1}$	$m\,s^{-1}$	$m\,s^{-1}$	$m\,s^{-1}$	$m\,s^{-1}$	$m\,s^{-1}$
0.3125	6.85	6.96	6.85	9.54	8.45	9.22
0.625	6.85	6.86	6.67	9.54	7.86	8.91
1.25	6.85	6.57	6.40	9.54	7.00	8.35
2.5	6.85	6.27	5.96	9.54	6.29	7.49
5.0	6.85	5.65	5.37	9.54	5.39	6.43
10.0	6.85	4.86	4.67	9.54	4.40	5.36

Table B1. day-time: This table shows all the capacity density scenarios modelled, associated number of turbines, park yields (WRF) modelled by Miller et al. (2015). It also shows the park yields estimated in this study using the standard approach, KEBA with a single boundary layer height (KEBA single) and KEBA with different average bay and night-time boundary layer heights (KEBA variable). The computed capacity factors, represented as fractions, from all the approaches are also included.

Capacity Density	Number of turbines	WRF	Standard	KEBA (fixed)	KEBA (variable)	WRF Capacity Factor	Standard Capacity Factor	KEBA fixed Capacity Factor	KEBA variable Capacity Factor
$MW_i\,km^{-2}$	-	$W_e\,m^{-2}$	$W_e\,m^{-2}$	$W_e\,m^{-2}$	$W_e\,m^{-2}$	-	-	-	-
0.3125	11700	0.06	0.06	0.06	0.06	0.20	0.19	0.19	0.18
0.625	23400	0.12	0.12	0.10	0.11	0.19	0.19	0.16	0.17
1.25	46800	0.22	0.24	0.18	0.19	0.17	0.19	0.14	0.15
2.5	93600	0.38	0.49	0.28	0.32	0.15	0.19	0.11	0.13
5.0	187200	0.56	0.97	0.39	0.47	0.11	0.19	0.08	0.09
10.0	374400	0.69	1.94	0.48	0.60	0.07	0.19	0.05	0.06

https://doi.org/10.5194/wes-2023-82
Preprint. Discussion started: 10 November 2023

eawe european academy of wind energy
Open Access WIND ENERGY SCIENCE DISCUSSIONS

Table C1. night-time: This table shows all the capacity density scenarios modelled, associated number of turbines, park yields (WRF) modelled by Miller et al. (2015). It also shows the park yields estimated in this study using the standard approach, KEBA with a single boundary layer height (KEBA single) and KEBA with different average bay and night-time boundary layer heights (KEBA variable). The computed capacity factors, represented as fractions, from all the approaches are also included.

Capacity Density	**Number of turbines**	**WRF**	**Standard**	**KEBA (fixed)**	**KEBA (variable)**	**WRF Capacity Factor**	**Standard Capacity Factor**	**KEBA fixed Capacity Factor**	**KEBA variable Capacity Factor**
$MW_i\,km^{-2}$	-	$W_e\,m^{-2}$	$W_e\,m^{-2}$	$W_e\,m^{-2}$	$W_e\,m^{-2}$	-	-	-	-
0.3125	11700	0.07	0.09	0.08	0.08	0.22	0.28	0.26	0.26
0.625	23400	0.12	0.18	0.16	0.16	0.20	0.28	0.26	0.25
1.25	46800	0.19	0.35	0.29	0.27	0.16	0.28	0.22	0.22
2.5	93600	0.30	0.71	0.48	0.43	0.12	0.28	0.20	0.17
5.0	187200	0.39	1.42	0.68	0.58	0.08	0.28	0.14	0.12
10.0	374400	0.41	2.84	0.85	0.68	0.04	0.28	0.05	0.07

Table D1. Undifferentiated: This table shows all the capacity density scenarios modelled, associated number of turbines, park yields (WRF) modelled by Miller et al. (2015). It also shows the park yields estimated in this study using the standard approach, KEBA with a single boundary layer height (KEBA single) and KEBA with different average bay and night-time boundary layer heights (KEBA variable). The computed capacity factors from all the approaches is also included.

Capacity Density	**Number of turbines**	**WRF**	**Standard**	**KEBA (fixed)**	**KEBA (variable)**	**WRF Capacity Factor**	**Standard Capacity Factor**	**KEBA fixed Capacity Factor**	**KEBA variable Capacity Factor**
$MW_i\,km^{-2}$	-	$W_e\,m^{-2}$	$W_e\,m^{-2}$	$W_e\,m^{-2}$	$W_e\,m^{-2}$	-	-	-	-
0.3125	11700	0.13	0.15	0.14	0.14	0.42	0.48	0.45	0.45
0.625	23400	0.24	0.30	0.26	0.26	0.39	0.48	0.42	0.42
1.25	46800	0.41	0.60	0.46	0.47	0.33	0.48	0.37	0.37
2.5	93600	0.68	1.19	0.78	0.75	0.27	0.48	0.30	0.31
5.0	187200	0.95	2.39	1.05	1.05	0.19	0.48	0.21	0.21
10.0	374400	1.10	4.78	1.30	1.28	0.11	0.48	0.13	0.13

https://doi.org/10.5194/wes-2023-82
Preprint. Discussion started: 10 November 2023

eawe european academy of wind energy
Open Access WIND ENERGY SCIENCE DISCUSSIONS

D1 Comparison with published numerical weather model-based estimates of technical wind energy potential

In Fig. 5, we have compared KEBA estimates of technical potential from our analysis with those performed independently by others over comparable regional and global scales using different numerical modelling approaches. For comparison in Kansas and Central USA we used the studies performed by Adams and Keith; Miller et al. and Volker et al. (Adams and Keith, 2013; Miller et al., 2015; Volker et al., 2017). From Volker et al., we only use their estimates for their largest deployment scenario ($10^5\ km^2$) in Central US. This was the most pertinent case for our analysis.

All three of these studies use a version of WRF to model the wind turbine yields and parametrize the wind turbines as momentum sinks. This means that they account for the fact that turbines extract momentum and kinetic energy from the wind thereby lowering wind speeds.While Miller et al. and Adams and Keithuse a variation of the Fitch scheme (Fitch et al., 2013b), Volker et al. use the extended wake parameterization or EWP scheme (Volker et al., 2015). The main difference between the Fitch scheme, its variation and the EWP is the while the latter does not include an explicit term to account for the Turbulent Kinetic Energy (TKE) generated by the turbine, the former 2 do. The different schemes lead to differences in the amount of mixing generated withing the boundary layer due to the turbine action. The Fitch scheme estimates more and the EWP relatively less, even though their estimates of wind speeds largely agree with each other(Volker et al., 2015).

It is important to appreciate these differences because Archer et al.(Archer et al., 2020) highlighted two bugs in implementation of the Fitch scheme in WRF versions prior to v4.2 that affect the Miller et al. study (Fischereit et al., 2021).It was shown that the additional term in the Fitch scheme adds excessive TKE and a coding bug prevents the TKE from being advected properly. Although preliminary analyses have shown that the two errors actually compensate for each other giving rise to TKE estimates that agree with observations (Archer et al., 2020; Larsén and Fischereit, 2021), it would be useful to briefly evaluate any potential impacts on our results and conclusions.

First, according to a review by Fischereit et al. the conclusions of neither of the 3 studies based used in this study,(Adams and Keith, 2013; Miller et al., 2015; Volker et al., 2015) are affected by the identified bug. Secondly, were these studies affected by the bug or the impact significant one would have expected a more prominent deviation between the Fitch based studies and the EWP based study. This is because the EWP schemes does not use the explicit TKE addition term with which the bug was related. Instead, it is observed that the different studies exhibit a similar trend of technical potential with installed capacity that culminates to a peak average of 1.1 W m^{-2}.

Further, the WRF trends in Kansas and Central US are consistent with previous studies that estimate global potentials. Relevant estimates of global land from Jacobson and Archer and Miller and Kleidon are shown in Fig. 6. These estimates and trends have been derived using global circulation models (GCMs). These are also unaffected by the errors in the Fitch scheme. These trends show the same variation in potentials as the WRF trends i.e. sub linear increase in potential beyond 1.5 MW $km^{-}2$ and culmination to a peak global average range of 0.2 - 0.6 W m^{-2} Miller et al. (2011); Miller and Kleidon (2016); Jacobson and Archer (2012); Wang and Prinn (2010, 2011); Marvel et al. (2012). The agreement between all the independent trends and regional and global scale highlights that the impact of the errors in the Fitch scheme are unlikely to affect the insights and conclusions generated from this study.

https://doi.org/10.5194/wes-2023-82
Preprint. Discussion started: 10 November 2023

eawe european academy of wind energy
Open Access WIND ENERGY SCIENCE DISCUSSIONS

D2 Technical Potential, Capacity Factors and Levelized Cost of Energy (LCOE)

Figure 6b shows that as the number of turbines deployed over the hypothetical wind farm area increases, the removal of kinetic energy (KE) reduces the capacity factor. This means that with the increasing deployed capacity , each turbine produces less energy than what it would have, had it been operating in isolation. The reduction in per turbine efficiency increases with increasing turbines. When the KE removal is neglected, the capacity factor remains unchanged (dotted gray line). While the addition of turbines generally increases the technical potential , the step-wise increments in generation reduce as the turbine numbers increase Fig. 6a. The lower increments are driven by the reductions in capacity factors Fig. 6b. The effect of this variation in capacity factors can be used to investigate their economic impacts using a standard economic cost metric known as the levelized cost of energy or LCOE (Ragheb, 2017). LCOE is represented by the following formula (Ragheb, 2017):

$$LCOE_{wind} = \frac{\sum_{t=1}^{n}(I_t + O\&M_t - PTC_t - D_t + T_t + R_t) \cdot \frac{1}{(1+i)^t}}{CF \cdot \sum_{t=0}^{t=n-1} P_t} \tag{D1}$$

In this equation, I_t and $O\&M_t$ refer to the capital and operations cost while PTC_t, D_T, T_t and R_t represent the credits, levies, taxes and royalties, respectively. The term $\frac{1}{(1+i)^t}$ is the present value factor which is used to account for the time value of money with a discount factor, i, over the lifespan of a wind farm. t represents a year within the operational period of a wind farm. CF is the capacity factor, which in this calculation would be different for different scenarios for WRF and KEBA but same for the standard approach. Since we are interested in simply illustrating only the economic impact of reductions in capacity factors due to KE removal, we can simplify Eq.(D1) such that LCOE is only a function of capacity factor. For this, we ignore tax related terms and assume that all costs and installed capacity terms (P_t) are sunk and installed at the once at the beginning of the operational life. The time factor also remains constant for all scenarios. It should be noted that this calculation is meant only to illustrate that capacity factor reduction arising from KE removal result in non-trivial increases in LCOE which highlights their inclusion into the policy design. In reality, turbine installation will occur over many years and so will the cost investments. A real LCOE calculation would need specific and quality controlled inputs about the timing and values of costs, levies and discount rates. With the simplification, Eq.(D1) would take the following form.

$$LCOE_{scenario} = \frac{1}{CF_{scenario}} \times constant \tag{D2}$$

In D2, the LCOE for each capacity density scenario is inversely related to the capacity factor. As the cost and installed capacity terms are same for the standard and the WRF and KEBA approaches, the percent change relative to the standard approach for each scenario can be calculated. These values for each of the installed capacity density scenarios are plotted for both WRF and KEBA estimates. For example, for the 2.5 MW km^{-2} case the standard approach assumes a 0.48 capacity factor while KEBA and WRF estimates 0.31 and 0.27. Then, to estimate the percent change relative to the standard approach the following approach is used:

https://doi.org/10.5194/wes-2023-82
Preprint. Discussion started: 10 November 2023

eawe european academy of wind energy
Open Access WIND ENERGY SCIENCE DISCUSSIONS

$$\%\,change\,in\,LCOE_{2.5} = \frac{LCOE_{2.5,\,KEBA/WRF} - LCOE_{2.5\,,standard}}{LCOE_{2.5\,,standard}} \tag{D3}$$

These values are tabulated in the table below.

Table E1. Tabulation of capacity factors estimated by KEBA, WRF and the standard approach along with the estimated change in LCOE (%) due to KE removal relative to the standard approach.

Capacity Density	**Number of turbines**	**WRF Capacity Factor**	**Standard Capacity Factor**	**KEBA variable Capacity Factor**	**WRF LCOE Change**	**KEBA variable LCOE Change**
$MW_i\,km^{-2}$	-	-	-	-	%	%
0.3125	11700	0.42	0.48	0.45	14	6
0.625	23400	0.39	0.48	0.42	23	14
1.25	46800	0.33	0.48	0.37	45	30
2.5	93600	0.27	0.48	0.31	77	54
5.0	187200	0.19	0.48	0.21	150	130
10.0	374400	0.11	0.48	0.13	430	270

The change in LCOE is only calculated for the installed capacity range from 0.3125 to 10 MW km^{-2} because this is the range that is typically assumed in wind energy policy scenarios. They show that as the capacity factor reduces the economic cost of wind energy goes up because each of the turbines performs less efficiently.

Author contributions. AK, JM and NTM designed the study. AK supervised the study while JM and NTM performed the analysis. JM wrote the manuscript. AK and NTM reviewed and edited the manuscript.

Competing interests. The authors declare that they have no conflict of interest.

Acknowledgements. I would like to thank Dr. Lee M. Miller for providing key scientific insights during the editing of the manuscript that have contributed greatly to improving it quality.

https://doi.org/10.5194/wes-2023-82
Preprint. Discussion started: 10 November 2023

eawe european academy of wind energy
Open Access WIND ENERGY SCIENCE DISCUSSIONS

References

U.S.EIA, https://www.eia.gov/state/seds/data.php?incfile=/state/seds/sep_use/tx/use_tx_KS.html&sid=KS, 2018.

Abkar, M., Sharifi, A., and Porté-Agel, F.: Large-eddy simulation of the diurnal variation of wake flows in a finite-size wind farm, Journal of Physics: Conference Series, 625, 012 031, https://doi.org/10.1088/1742-6596/625/1/012031, 2015.

Abkar, M., Sharifi, A., and Porté-Agel, F.: Wake flow in a wind farm during a diurnal cycle, Journal of Turbulence, 17, 420–441, https://doi.org/10.1080/14685248.2015.1127379, 2016.

Adams, A. S. and Keith, D. W.: Are global wind power resource estimates overstated?, Environmental Research Letters, 8, 015 021, https://doi.org/10.1088/1748-9326/8/1/015021, 2013.

Ahsbahs, T., Nygaard, N., Newcombe, A., and Badger, M.: Wind Farm Wakes from SAR and Doppler Radar, Remote Sensing, 12, https://doi.org/10.3390/rs12030462, 2020.

Aitken, M. L., Kosović, B., Mirocha, J. D., and Lundquist, J. K.: Large eddy simulation of wind turbine wake dynamics in the stable boundary layer using the Weather Research and Forecasting Model, Journal of Renewable and Sustainable Energy, 6, https://doi.org/10.1063/1.4885111, 2014.

Akhtar, N., Geyer, B., Rockel, B., Sommer, P. S., and Schrum, C.: Accelerating deployment of offshore wind energy alter wind climate and reduce future power generation potentials, Scientific Reports, 11, https://doi.org/10.1038/s41598-021-91283-3, 2021.

Archer, C. L. and Jacobson, M. Z.: Evaluation of global wind power, Journal of Geophysical Research: Atmospheres, 110, https://doi.org/https://doi.org/10.1029/2004JD005462, 2005.

Archer, C. L., Wu, S., Ma, Y., and Jiménez, P. A.: Two Corrections for Turbulent Kinetic Energy Generated by Wind Farms in the WRF Model, Monthly Weather Review, 148, 4823–4835, https://doi.org/10.1175/mwr-d-20-0097.1, 2020.

Badger, J., Kleidon, A., Imberger, M., Volker, P., Germer, S., Minz, J., and Deutsch, M.: Agora Energiewende, Agora Verkehrswende, Technical University of Denmark and Max-Planck-Institute for Biogeochemistry (2020): Making the Most of Offshore Wind: Re-Evaluating the Potential of Offshore Wind in the German North Sea., Tech. Rep. 176/01-S-2020/EN, Technical University of Denmark and Max Planck Institute of Biogeochemistry and Agora Energiewende, https://static.agora-energiewende.de/fileadmin/Projekte/2019/Offshore_Potentials/176_A-EW_A-VW_Offshore-Potentials_Publication_WEB.pdf, 2020.

Blahak, U. and Wetter-Jetzt: A Simple Parameterization of Drag Forces Induced by Large Wind Farms for Numerical Weather Prediction Models, https://api.semanticscholar.org/CorpusID:55966737, 2010.

Blanco, M. I.: The economics of wind energy, Renewable and Sustainable Energy Reviews, 13, 1372–1382, https://doi.org/10.1016/j.rser.2008.09.004, 2009.

Bodini, N., Zardi, D., and Lundquist, J. K.: Three-dimensional structure of wind turbine wakes as measured by scanning lidar, Atmospheric Measurement Techniques, 10, 2881–2896, https://doi.org/10.5194/amt-10-2881-2017, 2017.

Boettcher, M., Hoffmann, P., Lenhart, H.-J., Schlünzen, K. H., and Schoetter, R.: Influence of large offshore wind farms on North German climate, Meteorologische Zeitschrift, 24, 465–480, https://doi.org/10.1127/metz/2015/0652, 2015.

Brown, A., Beiter, P., Heimiller, D., Davidson, C., Denholm, P., Melius, J., Lopez, A., Hettinger, D., Mulcahy, D., and Porro, G.: Estimating Renewable Energy Economic Potential in the United States. Methodology and Initial Results, Tech. rep., https://doi.org/10.2172/1215323, 2016.

Capps, S. B. and Zender, C. S.: Estimated global ocean wind power potential from QuikSCAT observations, accounting for turbine characteristics and siting, Journal of geophysical research: atmospheres, 115, 2010.

https://doi.org/10.5194/wes-2023-82
Preprint. Discussion started: 10 November 2023

Cañadillas, B., Foreman, R., Barth, V., Siedersleben, S., Lampert, A., Platis, A., Djath, B., Schulz-Stellenfleth, J., Bange, J., Emeis, S., and Neumann, T.: Offshore wind farm wake recovery: Airborne measurements and its representation in engineering models, Wind Energy, 23, 1249–1265, https://doi.org/https://doi.org/10.1002/we.2484, 2020.

Christiansen, M. B. and Hasager, C. B.: Wake effects of large offshore wind farms identified from satellite SAR, Remote Sensing of Environment, 98, 251–268, https://doi.org/10.1016/j.rse.2005.07.009, 2005.

Corten, G. P.: Novel views on the extraction of energy from wind. Heat generation and terrain concentration, Energy research Centre of the Netherlands ECN, Petten, https://publicaties.ecn.nl/PdfFetch.aspx?nr=ECN-RX--01-054, european Wind Energy Conference 2001, Copenhagen(Denmark), 2-6 July 2001, ECN-RX-01-054, 2001.

Edenhofer, O., Pichs-Madruga, R., Sokona, Y., Seyboth, K., Matschoss, P., Kadner, S., Zwickel, T., Eickemeier, P., Hansen, G., Schlömer, S., et al.: IPCC special report on renewable energy sources and climate change mitigation, Prepared By Working Group III of the Intergovernmental Panel on Climate Change, Cambridge University Press, Cambridge, UK, 2011.

Enevoldsen, P., Permien, F.-H., Bakhtaoui, I., von Krauland, A.-K., Jacobson, M. Z., Xydis, G., Sovacool, B. K., Valentine, S. V., Luecht, D., and Oxley, G.: How much wind power potential does europe have? Examining european wind power potential with an enhanced socio-technical atlas, Energy Policy, 132, 1092–1100, https://doi.org/https://doi.org/10.1016/j.enpol.2019.06.064, 2019.

Eurek, K., Sullivan, P., Gleason, M., Hettinger, D., Heimiller, D., and Lopez, A.: An improved global wind resource estimate for integrated assessment models, Energy Economics, 64, https://doi.org/10.1016/j.eneco.2016.11.015, 2017.

Fischereit, J., Brown, R., Larsén, X. G., Badger, J., and Hawkes, G.: Review of Mesoscale Wind-Farm Parametrizations and Their Applications, Boundary-Layer Meteorology, 182, 175–224, https://doi.org/10.1007/s10546-021-00652-y, 2021.

Fitch, A. C., Olson, J. B., Lundquist, J. K., Dudhia, J., Gupta, A. K., Michalakes, J., and Barstad, I.: Local and Mesoscale Impacts of Wind Farms as Parameterized in a Mesoscale NWP Model, Monthly Weather Review, 140, 3017–3038, https://doi.org/10.1175/mwr-d-11-00352.1, 2012.

Fitch, A. C., Lundquist, J. K., and Olson, J. B.: Mesoscale Influences of Wind Farms throughout a Diurnal Cycle, Monthly Weather Review, 141, 2173–2198, https://doi.org/10.1175/mwr-d-12-00185.1, 2013a.

Fitch, A. C., Olson, J. B., and Lundquist, J. K.: Parameterization of Wind Farms in Climate Models, Journal of Climate, 26, 6439 – 6458, https://doi.org/10.1175/JCLI-D-12-00376.1, 2013b.

Frandsen, S., Barthelmie, R., Pryor, S., Rathmann, O., Larsen, S., Højstrup, J., and Thøgersen, M.: Analytical modelling of wind speed deficit in large offshore wind farms, Wind Energy: An International Journal for Progress and Applications in Wind Power Conversion Technology, 9, 39–53, 2006.

GEA: Global Energy Assessment: Toward a Sustainable Future, Cambridge University Press, https://doi.org/10.1017/CBO9780511793677, 2012.

Gustavson, M. R.: Limits to Wind Power Utilization, Science, 204, 13–17, https://doi.org/10.1126/science.204.4388.13, 1979.

Hasager, C., Vincent, P., Badger, J., Badger, M., Bella, A. D., Peña, A., Husson, R., and Volker, P.: Using Satellite SAR to Characterize the Wind Flow around Offshore Wind Farms, Energies, 8, 5413–5439, https://doi.org/10.3390/en8065413, 2015.

Hoogwijk, M., de Vries, B., and Turkenburg, W.: Assessment of the global and regional geographical, technical and economic potential of onshore wind energy, Energy Economics, 26, 889–919, https://doi.org/https://doi.org/10.1016/j.eneco.2004.04.016, 2004.

IEA: World energy outlook 2021 – analysis, https://www.iea.org/reports/world-energy-outlook-2021, 2021.

Jacobson, M. Z. and Archer, C. L.: Saturation wind power potential and its implications for wind energy, Proceedings of the National Academy of Sciences, 109, 15 679–15 684, https://doi.org/10.1073/pnas.1208993109, 2012.

https://doi.org/10.5194/wes-2023-82
Preprint. Discussion started: 10 November 2023

Jacobson, M. Z. and Delucchi, M. A.: Providing all global energy with wind, water, and solar power, Part I: Technologies, energy resources, quantities and areas of infrastructure, and materials, Energy Policy, 39, 1154–1169, https://doi.org/https://doi.org/10.1016/j.enpol.2010.11.040, 2011.

Katic, I., Højstrup, J., and Jensen, N. O.: A simple model for cluster efficiency, in: European wind energy association conference and exhibition, vol. 1, pp. 407–410, A. Raguzzi Rome, Italy, 1986.

Kleidon, A.: Physical limits of wind energy within the atmosphere and its use as renewable energy: From the theoretical basis to practical implications, Meteorologische Zeitschrift, https://doi.org/10.1127/metz/2021/1062, 2021.

Kleidon, A. and Miller, L. M.: The Kinetic Energy Budget of the Atmosphere (KEBA) model 1.0: a simple yet physical approach for estimating regional wind energy resource potentials that includes the kinetic energy removal effect by wind turbines, Geoscientific Model Development, 13, 4993–5005, https://doi.org/10.5194/gmd-13-4993-2020, 2020.

Larsén, X. G. and Fischereit, J.: A case study of wind farm effects using two wake parameterizations in the Weather Research and Forecasting (WRF) model (V3.7.1) in the presence of low-level jets, Geoscientific Model Development, 14, 3141–3158, https://doi.org/10.5194/gmd-14-3141-2021, 2021.

Lopez, A., Roberts, B., Heimiller, D., Blair, N., and Porro, G.: Tech. rep., National Renewable Energy Laboratory, https://doi.org/https://doi.org/10.2172/1047328, 2012.

Lu, X., McElroy, M. B., and Kiviluoma, J.: Global potential for wind-generated electricity, Proceedings of the National Academy of Sciences, 106, 10 933–10 938, https://doi.org/10.1073/pnas.0904101106, 2009.

Lundquist, J. K., Takle, E. S., Boquet, M., Kosovic, B., Rhodes, M. E., Rajewski, D., Doorenbos, R., Irvin, S., Aitken, M. L., Friedrich, K., et al.: Lidar observations of interacting wind turbine wakes in an onshore wind farm, in: EWEA meeting proceedings, pp. 10–13, 2014.

Lundquist, J. K., DuVivier, K. K., Kaffine, D., and Tomaszewski, J. M.: Costs and consequences of wind turbine wake effects arising from uncoordinated wind energy development, Nature Energy, 4, 26–34, https://doi.org/10.1038/s41560-018-0281-2, 2018.

Maas, O. and Raasch, S.: Wake properties and power output of very large wind farms for different meteorological conditions and turbine spacings: A large-eddy simulation case study for the German Bight, https://doi.org/10.5194/wes-2021-83, 2021.

Manwell, J. F., McGowan, J. G., and Rogers, A. L.: Wind energy explained, John Wiley & Sons, Nashville, TN, 2 edn., 2010.

Marvel, K., Kravitz, B., and Caldeira, K.: Geophysical limits to global wind power, Nature Climate Change, 3, 118–121, https://doi.org/10.1038/nclimate1683, 2012.

McKenna, R., Pfenninger, S., Heinrichs, H., Schmidt, J., Staffell, I., Bauer, C., Gruber, K., Hahmann, A. N., Jansen, M., Klingler, M., Landwehr, N., Larsén, X. G., Lilliestam, J., Pickering, B., Robinius, M., Tröndle, T., Turkovska, O., Wehrle, S., Weinand, J. M., and Wohland, J.: High-resolution large-scale onshore wind energy assessments: A review of potential definitions, methodologies and future research needs, Renewable Energy, 182, 659–684, https://doi.org/10.1016/j.renene.2021.10.027, 2022.

Miller, L. and Kleidon, A.: Wind speed reductions by large-scale wind turbine deployments lower turbine efficiencies and set low generation limits, Proceedings of the National Academy of Sciences, 113, 13 570–13 575, https://doi.org/10.1073/pnas.1602253113, 2016.

Miller, L., Brunsell, N. A., Mechem, D. B., Gans, F., Monaghan, A. J., Vautard, R., Keith, D. W., and Kleidon, A.: Two methods for estimating limits to large-scale wind power generation, Proceedings of the National Academy of Sciences, 112, 11 169–11 174, https://doi.org/10.1073/pnas.1408251112, 2015.

Miller, L. M. and Keith, D. W.: Observation-based solar and wind power capacity factors and power densities, Environmental Research Letters, 13, 104 008, https://doi.org/10.1088/1748-9326/aae102, 2018.

https://doi.org/10.5194/wes-2023-82
Preprint. Discussion started: 10 November 2023

Miller, L. M., Gans, F., and Kleidon, A.: Estimating maximum global land surface wind power extractability and associated climatic consequences, Earth System Dynamics, 2, 1–12, https://doi.org/10.5194/esd-2-1-2011, 2011.

Mirocha, J. D., Rajewski, D. A., Marjanovic, N., Lundquist, J. K., Kosović, B., Draxl, C., and Churchfield, M. J.: Investigating wind turbine impacts on near-wake flow using profiling lidar data and large-eddy simulations with an actuator disk model, Journal of Renewable and Sustainable Energy, 7, https://doi.org/10.1063/1.4928873, 2015.

Méchali, M., Barthelmie, R., Frandsen, S., Jensen, L., and Réthoré, P.-E.: Wake effects at Horns Rev and their influence on energy production, 2006.

Nygaard, N. G. and Newcombe, A. C.: Wake behind an offshore wind farm observed with dual-Doppler radars, Journal of Physics: Conference Series, 1037, 072 008, https://doi.org/10.1088/1742-6596/1037/7/072008, 2018.

Nygaard, N. G., Steen, S. T., Poulsen, L., and Pedersen, J. G.: Modelling cluster wakes and wind farm blockage, Journal of Physics: Conference Series, 1618, 062 072, https://doi.org/10.1088/1742-6596/1618/6/062072, 2020.

Pedersen, J. G., Svensson, E., Poulsen, L., and Nygaard, N. G.: Turbulence Optimized Park model with Gaussian wake profile, Journal of Physics: Conference Series, 2265, 022 063, https://doi.org/10.1088/1742-6596/2265/2/022063, 2022.

Peixoto, J. P. and Oort, A. H.: Physics of climate, Springer, 1992.

Platis, A., Siedersleben, S. K., Bange, J., Lampert, A., Bärfuss, K., Hankers, R., Cañadillas, B., Foreman, R., Schulz-Stellenfleth, J., Djath, B., Neumann, T., and Emeis, S.: First in situ evidence of wakes in the far field behind offshore wind farms, Scientific Reports, 8, https://doi.org/10.1038/s41598-018-20389-y, 2018.

Prakash, G., Anuta, H., Gielen, D., Gorini, R., Wagner, N., and Gallina, G.: Future of wind:Deployment, investment, technology, grid integration and socio-economic aspects (A Global Energy Transformation paper), Tech. Rep. ISBN 978-92-926-155-3, International Renewable Energy Agency, https://www.irena.org/-/media/Files/IRENA/Agency/Publication/2019/Oct/IRENA_Future_of_wind_2019.pdf, 2019.

Ragheb, M.: Chapter 25 - Economics of Wind Power Generation, in: Wind Energy Engineering, edited by Letcher, T. M., pp. 537–555, Academic Press, https://doi.org/https://doi.org/10.1016/B978-0-12-809451-8.00025-4, 2017.

Rajewski, D. A., Takle, E. S., Lundquist, J. K., Oncley, S., Prueger, J. H., Horst, T. W., Rhodes, M. E., Pfeiffer, R., Hatfield, J. L., Spoth, K. K., and Doorenbos, R. K.: Crop Wind Energy Experiment (CWEX): Observations of Surface-Layer, Boundary Layer, and Mesoscale Interactions with a Wind Farm, Bulletin of the American Meteorological Society, 94, 655–672, https://doi.org/10.1175/bams-d-11-00240.1, 2013.

Ruijgrok, E., Bulder, B., and Druten, E. v.: Cost Evaluation of North Sea Offshore Wind Post 2030, Wittveen+Bos, 2019.

Schallenberg-Rodriguez, J.: A methodological review to estimate techno-economical wind energy production, Renewable and Sustainable Energy Reviews, 21, 272–287, https://doi.org/https://doi.org/10.1016/j.rser.2012.12.032, 2013.

Schneemann, J., Rott, A., Dörenkämper, M., Steinfeld, G., and Kühn, M.: Cluster wakes impact on a far-distant offshore wind farm's power, Wind Energy Science, 5, 29–49, https://doi.org/10.5194/wes-5-29-2020, 2020.

Siedersleben, S. K., Platis, A., Lundquist, J. K., Lampert, A., Bärfuss, K., Cañadillas, B., Djath, B., Schulz-Stellenfleth, J., Bange, J., Neumann, T., and Emeis, S.: Evaluation of a wind farm parametrization for mesoscale atmospheric flow models with aircraft measurements, Meteorol. Z., 27, 401–415, 2018.

Skamarock, W., Klemp, J., Dudhia, J., Gill, D., Barker, D., Wang, W., Huang, X.-Y., and Duda, M.: A Description of the Advanced Research WRF Version 3, Tech. rep., https://doi.org/10.5065/D68S4MVH, 2008.

Staffell, I. and Pfenninger, S.: Using bias-corrected reanalysis to simulate current and future wind power output, Energy, 114, 1224–1239, https://doi.org/10.1016/j.energy.2016.08., 2016.

https://doi.org/10.5194/wes-2023-82
Preprint. Discussion started: 10 November 2023

Stull, R. B.: An Introduction to Boundary Layer Meteorology, vol. 13, Springer, 1 edn., 2009.

Trier, S., Davis, C., and Ahijevych, D.: Environmental controls on the simulated diurnal cycle of warm-season precipitation in the continental United States, Journal of the atmospheric sciences, 67, 1066–1090, 2010.

Volker, P., Hahmann, A., Badger, J., and Ejsing Jørgensen, H.: Prospects for generating electricity by large onshore and offshore wind farms: Letter, Environmental Research Letters, 12, https://doi.org/10.1088/1748-9326/aa5d86, open Access - Original content from this work may be used under the terms of the Creative Commons Attribution 3.0 licence. Any further distribution of this work must maintain attribution to the author(s) and the title of the work, journal citation and DOI., 2017.

Volker, P. J. H., Badger, J., Hahmann, A. N., and Ott, S.: The Explicit Wake Parametrisation V1.0: a wind farm parametrisation in the mesoscale model WRF, Geoscientific Model Development, 8, 3715–3731, https://doi.org/10.5194/gmd-8-3715-2015, 2015.

Wang, C. and Prinn, R. G.: Potential climatic impacts and reliability of very large-scale wind farms, Atmospheric Chemistry and Physics, 10, 2053–2061, 2010.

Wang, C. and Prinn, R. G.: Potential climatic impacts and reliability of large-scale offshore wind farms, Environmental Research Letters, 6, 025 101, 2011.

Wiser, R., Jenni, K., Seel, J., Baker, E., Hand, M., Lantz, E., and Smith, A.: Expert elicitation survey on future wind energy costs, Nature Energy, 1, https://doi.org/10.1038/nenergy.2016.135, 2016.

Wu, Y.-T. and Porté-Agel, F.: Modeling turbine wakes and power losses within a wind farm using LES: An application to the Horns Rev offshore wind farm, Renewable Energy, 75, 945–955, https://doi.org/10.1016/j.renene.2014.06.019, 2015.